Prmt5 promotes vascular morphogenesis independently of its methyltransferase activity.

Aurélie Quillien[1*], Manon Boulet[1,2], Séverine Ethuin[1], Laurence Vandel[1,2*]

[1]Centre de Biologie du Développement (CBD), Centre de Biologie Intégrative (CBI), Université de Toulouse, CNRS, UPS, France

[2]Current affiliation : Université Clermont Auvergne, CNRS, Inserm, GReD, F-3000 Clermont-Ferrand, France

*Corresponding Authors

Aurélie Quillien (aurelie.quillien@gmail.com)

Laurence Vandel (laurence.vandel@uca.fr)

ABSTRACT

During development, the vertebrate vasculature undergoes major growth and remodeling. While the transcriptional cascade underlying blood vessel formation starts to be better characterized, little is known concerning the role and mode of action of epigenetic enzymes during this process. Here, we explored the role of the Protein Arginine Methyl Transferase Prmt5 during blood vessel formation and hematopoiesis in zebrafish. Through the generation of a *prmt5* mutant, we highlighted a key role of Prmt5 in both hematopoiesis and blood vessel formation. Notably, we showed that Prmt5 promotes vascular morphogenesis through the transcriptional control of ETS transcription factors and adhesion proteins in endothelial cells. Interestingly, we found that Prmt5 methyltransferase activity is not required to regulate gene expression, and the comparison of chromatin architecture impact on reporter genes expression leads us to propose that Prmt5 rather regulates transcription by acting as a scaffold protein that facilitates chromatin looping in these cells.

Key words

Prmt5; zebrafish; angiogenesis; hematopoiesis; endothelial cells; chromatin looping

48 **INTRODUCTION**

49 Blood vessel formation is an essential developmental process required for the survival of all
50 vertebrates and much effort has been devoted to understand the molecular pathways and to
51 identify key molecules that regulate different aspects of this process. Interestingly, the vascular
52 anatomy and the mechanisms involved in vessel formation are highly conserved among
53 vertebrates (for a review, (Isogai et al., 2001)). Hence, in the past two decades, zebrafish has
54 been proven to be a useful model to study vascular morphogenesis and blood cell formation
55 *in vivo* (Beis and Stainier, 2006; Lawson and Weinstein, 2002a; Thisse and Zon, 2002).

56 In vertebrates, blood cell formation is tightly associated with the development of the vascular
57 system. Hematopoietic Stem Cells (HSC), which give rise to the different blood cell lineages,
58 emerge directly from the ventral part of the dorsal aorta, an area referred to as the hemogenic
59 endothelium. Notably, the ETS transcription factor ETV2 functions as a master regulator for
60 the formation of endothelial and hematopoietic cell lineages through the induction of both blood
61 cells and vasculature transcriptional programs, in mouse and in zebrafish (Liu et al., 2015b;
62 Wong et al., 2009). In endothelial cells, ETV2 regulates the expression of other ETS
63 transcription factors, VEGF (Vascular Endothelial Growth factor) signaling receptors and
64 effectors, Rho-GTPases and adhesion molecules (Liu et al., 2015b; Wong et al., 2009).
65 Besides, adhesion molecules have been shown to be crucial players in vascular
66 morphogenesis as Vascular Endothelial cadherin (VE-cad/ cdh5) and endothelial cell-selective
67 adhesion molecule (Esama) are essential for junction remodeling and blood vessel elongation
68 in zebrafish (Sauteur et al., 2017; Sauteur et al., 2014). Indeed, loss of function of both *cdh5*
69 and *esama* leads to the formation of disconnected vessels and delayed lumen formation.
70 Likewise, knock down of the scaffold protein Amolt2, which associates to VE-cadherin, also
71 leads to sprout elongation defects and narrowed aortic lumen (Hultin et al., 2014). While the
72 transcriptional cascade underlying blood vessel formation starts to be better characterized,
73 little is known concerning the role and mode of action of epigenetic enzymes during this
74 process. Even though chromatin-modifying enzymes have been described as central in

75 cardiovascular disease and development (Rosa-Garrido et al., 2018; Shailesh et al., 2018),
76 only few examples illustrate in detail the role of epigenetic enzymes during blood vessel
77 development. For instance, the chromatin-remodeling enzyme BRG1 affects early vascular
78 development as well as hematopoiesis in mice (Griffin et al., 2008), and the histone
79 acetyltransferase P300 has been proposed to be recruited at the promoter of specific
80 endothelial genes by the ETS transcription factor ERG (ETS Related Gene) to control their
81 expression both *in vivo* in zebrafish and in HUVEC (Human Umbilical Vein Endothelial Cell)
82 (Fish et al., 2017; Kalna et al., 2019).

83 Given the common origin of blood and endothelial cells, and their partially shared
84 transcriptional programs, it is plausible that known chromatin-modifying enzymes affecting
85 hematopoiesis could also control blood vessel formation. Along this line, the epigenetic
86 enzyme Prmt5 (Protein Arginine Methyltransferase 5) has been identified as a key player in
87 blood cell formation (Liu et al., 2015a) but its impact on endothelial development has not been
88 investigated to date. Prmt5 catalyzes the symmetric di-methylation of arginine residues on a
89 variety of proteins including histones and therefore acts on many cellular processes such as
90 genome organization, transcription, differentiation, cell cycle regulation or spliceosome
91 assembly, among others (Blanc and Richard, 2017; Karkhanis et al., 2011; Stopa et al., 2015).
92 Prmt5 is mainly known to repress transcription through the methylation of arginine residues on
93 histones H3 and H4 and has been shown to regulate several differentiation processes such as
94 myogenesis, oligodendrocyte and germ cell differentiation or hematopoiesis (Batut et al., 2011;
95 Liu et al., 2015a; Shailesh et al., 2018; Zhu et al., 2019). In mice, *prmt5* knock out prevents
96 pluripotent cells to form from the inner cell mass and is embryonic lethal (Tee et al., 2010).
97 Conditional loss of *prmt5* in mice leads to severe anemia and pancytopenia and Prmt5
98 maintains Hematopoietic Stem Cells (HSCs) and ensures proper blood cell progenitor
99 expansion (Liu et al., 2015a). Loss of *prmt5* leads to oxidative DNA damages, increased cell
100 apoptosis due to p53 dysregulation and as a consequence, to HSC exhaustion. In this context,

101 Prmt5 protects HSCs from DNA damages by allowing the splicing of genes involved in DNA
102 repair (Tan et al., 2019).

103 Here, we explored the role of the Protein Arginine MethylTransferase Prmt5 during blood
104 vessel formation and in hematopoiesis in zebrafish. Through the generation of a *prmt5* mutant,
105 we highlight the key role of this gene during vascular morphogenesis *via* the control of
106 expression of several ETS transcription factors and adhesion molecules. Moreover, we show
107 that Prmt5 methyltransferase activity is not required for blood vessel formation and our results
108 suggest that Prmt5 helps to shape correct chromatin conformation in endothelial cells.

109

110 **RESULTS**

111 ***Prmt5 is required for HSC maintenance and lymphoid progenitor expansion***

112 To characterize *prmt5* function, we generated a *prmt5* mutant by targeting the second exon of
113 *prmt5* with the CRISPR/Cas9 system. A deletion of 23 nucleotides was obtained, leading to a
114 premature stop codon before the catalytic domain of Prmt5 (Fig. 1A). As a consequence,
115 Prmt5, which was expressed ubiquitously in the trunk at 24 hours post fertilization (hpf), was
116 no longer detected in the mutant (Fig. 1B, C). Similarly, Prmt5 expression was severely
117 reduced in *prmt5* morpholino-injected embryos as compared to control morphants (Fig. S1 A,
118 B) (Batut et al., 2011). In order to test whether Prmt5 regulates hematopoiesis in zebrafish,
119 we took advantage of the transgenic line *Tg*(*gata2b:Gal4;UAS:lifeactGFP)* that labels
120 Hematopoietic Stem Cells (HSCs) (Butko et al., 2015). HSCs emerge from the ventral wall of
121 the dorsal aorta (DA, Fig. 1D, D'), before migrating into the Caudal Hematopoietic Tissue
122 (CHT) (Fig. 1D) where Hematopoietic Stem and Progenitor Cells (HSPCs) proliferate and
123 undergo maturation (Butko et al., 2015). Reminiscent of the data published in mice (Liu et al.,
124 2015a), the loss of *prmt5* led to an increased number of *gata2b*+ HSCs in 36 hpf mutant
125 embryos as compared to wild type ones (Fig. 1E-G). In addition, we found that the relative
126 expression of *scla*, *runx1* or *cmyb,* which are specifically expressed in emerging HSCs, was

127 increased in *prmt5* mutant embryos as compared to wild type embryos (Fig. 1H). These results
128 suggest that Prmt5 regulates the number of emerging HSCs from the dorsal aorta. We next
129 investigated whether blood cell formation was impaired in *prmt5* zebrafish mutant as described
130 in mouse (Liu et al., 2015a). HSPCs give rise to different blood cell progenitors, such as
131 lymphoid progenitors which colonize the thymus leading to T lymphopoiesis (Fig. 1D) (Ma et
132 al., 2013). As *gata2b*+ lymphoid progenitors deriving from *gata2b*+ HSCs can be detected in
133 the thymus of transgenic zebrafish larvae from day 3 (Butko et al., 2015), we investigated
134 whether Prmt5 could act on theses progenitors. Indeed, we found that at 5 days, the number
135 of *gata2b*+ *lymphoid* progenitors in the thymus was significantly reduced in *prmt5* mutant and
136 in morphant embryos as compared to wild type embryos (Fig. 1I-K, Fig. S1 C, D, G),
137 suggesting that Prmt5 is required for lymphoid progenitor expansion. Altogether, these data
138 indicate an important and conserved role of Prmt5 during hematopoiesis in zebrafish as in
139 mouse.

140 ***Prmt5 is required for vascular morphogenesis***

141 As Prmt5 regulates zebrafish hematopoiesis, we next asked whether Prmt5 could also play a
142 role during blood vessel formation, either during angiogenesis or vasculogenesis. First, we
143 analyzed the expression and localization of Prmt5 by immunostaining in *Tg(fli1a:eGFP)*
144 transgenic embryos, in which endothelial cells can be visualized with *egfp* (Lawson and
145 Weinstein, 2002b). We found that Prmt5 was clearly expressed in early endothelial cells at 14
146 somite stage (Fig. 2A-A''). At 24 hpf, Prmt5 was expressed in endothelial cells of the dorsal
147 aorta (DA) and of the cardinal vein (CV) (Fig. 2B, B', D). Prmt5 was also detected in
148 Intersegmental Vessels (ISVs) sprouting from the DA, in either the tip cell (leading the sprout)
149 or the stalk cell (Fig. 2C, C', D). We then analyzed whether blood vessel formation was affected
150 in transgenic *Tg(fli1a:eGFP) prmt5* mutants at 28 hpf. We found that the dorsal aorta diameter
151 of mutant embryos was reduced as compared to the control (Fig. 2D, E, F close-ups),
152 suggesting that lumen formation was perturbed. To confirm this result, we made use of the
153 Notch reporter line *Tg(TP1bglob:VenusPEST)*^{s940} in which only the dorsal aorta cells express

154 the transgene while the cardinal vein endothelial cells do not (Ninov et al., 2012; Quillien et al.,
155 2014). In this transgenic context the area occupied by the dorsal aorta in *prmt5* morphant
156 embryos was significantly reduced as compared to control embryos (Fig. 2G-I). *Prmt5* mutant
157 embryos also showed a defect of sprouting ISV to reach the most dorsal part of the trunk and
158 to connect with other ISVs and form the Dorsal Longitudinal Anastomotic Vessel (DLAV) (Fig.
159 2D, E, F). This defect was associated with a significant reduction of ISV length (Fig. 2E, F, K)
160 but with no impact on the number of endothelial cells (Fig. 2J). The observed size reduction of
161 ISVs is thus most likely the result of an elongation issue rather than a proliferation defect. Of
162 note, *prmt5* morphants reproduced the phenotype observed in *prmt5* mutants *i.e.* a reduced
163 ISV length at 28 hpf (Fig. S2 A-D).

164 To get a better insight into the impact of Prmt5 on the dynamics of vascular system formation,
165 we performed time-lapse analyses in control and *prmt5* morphant embryos. Time-lapse
166 confocal movies were carried out from 28 hpf to 38 hpf to follow the elongation of ISVs to the
167 formation of an effective lumen. As compared to control morphants, *prmt5* morphants showed
168 an impaired formation of ISV lumen and DLAV. Indeed, *in prmt5* morphants tip cells failed to
169 stay connected to the stalk cells and to contact other tip cells to allow the formation of the
170 DLAV (Fig. 3A-B). Moreover, supernumerary connections were detected in the context of
171 *prmt5*-loss of function (Fig. 3B). Altogether, these data suggest a central role for Prmt5 in
172 vascular morphogenesis.

173 The master gene regulator ETV2, ETS transcription factors and adhesion proteins have been
174 shown to be involved in blood vessel formation (Craig et al., 2015; Hultin et al., 2014; Pham et
175 al., 2007; Sauteur et al., 2017; Sauteur et al., 2014). Analyzing single cell RNA-sequencing
176 data from Wagner et al. (Wagner et al., 2018), allowed us to determine that *prmt5* is expressed
177 in endothelial cells at 10 hpf (like *etv2* and *fli1a*) and that its expression decreases in later
178 stages, when the expression of *fli1b*, *cdh5*, *agtr2*, *esama*, and *amotl2a* starts to increase (Fig.
179 S3). To test whether Prmt5 could regulate the expression of these genes, we performed RT-
180 qPCR experiments on mutant embryos and on their wild type counterparts. While we found

181 that *etv2* expression was not affected, the expression of ETS transcription factors (*fli1a, fli1b*)
182 and adhesion proteins *(cdh5*, *agtr2*, *esama* and *amotl2a),* all putative ETV2 target genes (Liu
183 et al., 2015b; Wong et al., 2009), was significantly reduced in *prmt5* mutant (Fig. 3C). Of note,
184 we also detected a reduction of *fli1a* and *cdh5* expression in *prmt5* mutant by *in situ*
185 hybridization (Fig. S4). As *etv2* expression was unaffected by the loss of *prmt5* but its targets
186 were down-regulated, it is tempting to speculate that Prmt5 could modulate ETV2 activity at
187 post-translational level.

188 ***Prmt5 methyltransferase activity is not required for vascular morphogenesis***

189 That Prmt5 modulates gene expression by methylating a variety of proteins including histones
190 but also transcription (co)factors led us to test whether Prmt5 methyltransferase activity was
191 required for vascular morphogenesis and lymphoid progenitor formation. To this end, *prmt5*
192 mutant or morphant embryos were injected with wild type *human prmt5* mRNA (*hprmt5WT*) or
193 with a catalytic mutant form of this mRNA (*hprmt5MUT*) (Pal et al., 2003). In mice, the
194 expansion of lymphoid progenitor relies on Prmt5 methyltransferase activity (Liu et al., 2015a).
195 Consistent with this, *hprmt5WT* but not *prmt5MU*T mRNA, was able to restore normal lymphoid
196 progenitor expansion in *prmt5* morphant embryos (Fig. S1 C-G). This underscores the
197 conserved requirement of PRMT5 methyltransferase activity for lymphoid progenitor formation
198 in human and zebrafish. We then tested whether the same was true for ISV elongation and the
199 expression of *etv2* target genes. Surprisingly, we found that both mRNAs were able to restore
200 ISV elongation, albeit to a slightly different extend, as indicated by the average ISV length in
201 injected mutant embryos as compared to non-injected mutants (Fig. 4A-E). Indeed, we
202 observed that the average length of ISVs in *hprmt5WT*-injected mutants was even longer than
203 intersegmental vessels of wild type embryos, while the average length in *hprmt5MUT* injected
204 mutants was significantly superior to non-injected mutants but shorter than control embryos
205 (Fig. 4 E). Interestingly, no difference could be seen in the cell number per ISV in the different
206 contexts (Fig. 4F) thus ruling out the possibility that Prmt5 regulates cell proliferation at the
207 ISV. Finally, RT-qPCR experiments revealed that both *hprmt5WT* and *hprmt5MUT* mRNAs

208 were able to restore the expression of *etv2* target genes, except for *fli1a* whose expression
209 was only rescued by *hprmt5WT* (Fig. 4G). In sum, these results indicate that Prmt5
210 methyltranferase activity is largely dispensable for its function in blood vessel formation.

211 ***Prmt5 might help to shape correct chromatin conformation in endothelial cells***

212 As Prmt5 methyltransferase activity seems to be not required for gene expression regulation
213 in vascular morphogenesis, we speculated that Prmt5 could act as a scaffold protein in
214 complexes mediating transcription and chromatin looping. Indeed, Prmt5 has been proposed
215 to promote enhancer-promoter looping at the PPARγ2 locus and more broadly to facilitate
216 chromatin connection in adipocytes, *via* the recruitments of Mediator subunit MED1 and
217 SWI/SNF chromatin remodeling complex subunit Brg1 ATPase (LeBlanc et al., 2016). Thus,
218 we decided to inspect the chromatin architecture of the flanking region of identified Prmt5-
219 regulated genes using ATAC-seq data from zebrafish endothelial cells that we previously
220 generated (Quillien et al., 2017). Doing so, we found that putative enhancers are on average
221 distant of 16 kb from the transcriptional start site (TSS) (Table S1, Figure S5), indicating that
222 their expression could rely on proper chromatin looping. To further characterize these specific
223 *cis* regulatory regions, we turned into the mouse model and analyzed the ChIP-seq data of
224 Etv2 and Prmt5-dependent H4R3 di-methylation to determine whether Prmt5 target genes
225 identified in our study were conserved in mouse (Girardot et al., 2014; Liu et al., 2015a). We
226 found that Etv2 is recruited to the cis regulatory element of *amotl2*, *cdh5* and *fli1* (Table 1) and
227 that its binding was associated with the presence of H4R3me2 for some of them, suggesting
228 that ETV2 and Prmt5 can be recruited on the same regions in mouse. In order to gain further
229 insight into the potential role of Prmt5 in supporting proper chromatin conformation in
230 endothelial cells, we analyzed and compared the expression of *Gal4* reporter genes in an
231 endogenous (Fig. 5A) and in an artificial chromatin context (Fig. 5E). The first construction
232 used consists in the transgenic line *TgBAC(cdh5:GAL4FF);Tg(UAS:GFP)* that contains the
233 sequence of an optimized version of Gal4VP16 (*GAL4FF*) inserted at the TSS of *cdh5* gene
234 between *cdh5* promoter region (P) and a putative enhancer (E) distant of ~20kb as defined by

235 the presence of two ATAC-seq positive regions (Table S1, Fig. 5A, Fig. S5) (Bussmann and
236 Schulte-Merker, 2011; Quillien et al., 2017). Therefore, in double transgenic individuals, the
237 level of GFP fluorescence intensity correlates with endogenous *cdh5* expression. In addition,
238 we generated a transgenic line where the *cdh5* promoter and putative enhancer were cloned
239 next to each other, both upstream of the *Gal4VP16* coding sequence (Fig. 5E). In double
240 transgenic embryos *Tg(cdh5:Gal4VP16); Tg(UAS:KAEDE),* the fluorescence intensity of the
241 protein KAEDE is an artificial read out of *cdh5* transcription for which chromatin looping is not
242 required. Comparing the level of fluorescence intensity in
243 *TgBAC(cdh5:GAL4FF);Tg(UAS:GFP)* transgenic line in control condition and in the context of
244 *prmt5* knock down, we observed a strong reduction of GFP fluorescence intensity in *prmt5*
245 morphants (Fig. 5B-D), indicating that Prmt5 is required for *cdh5* expression in an endogenous
246 context. In double transgenic embryos *Tg(cdh5:Gal4VP16); Tg(UAS:KAEDE)*, the fluorescent
247 protein KAEDE was expressed in blood vessels (Fig. 5F), validating that the putative enhancer
248 and the promotor region of *cdh5* are sufficient to drive gene expression in endothelial cells.
249 However, in this artificial context, *prmt5* morpholino injection had no effect on the level of
250 KAEDE fluorescence intensity as compared to control morphants (Fig. 5F-H). This result
251 suggests that in this particular context *i.e.* when chromatin looping between enhancer and
252 promoter was not needed, Prmt5 was not required either for gene expression. This finding
253 supports the idea that Prmt5 plays a role in the formation of the correct 3D environment for
254 endothelial genes expression. Finally, rescue experiments were performed by injecting either
255 wild type or a catalytic mutant of human *prmt5* mRNA to determine whether Prmt5
256 methyltransferase activity was required for the transcriptional control of *cdh5* expression in the
257 endogenous context. We found that both wild type and mutant *hprmt5* mRNAs restored GFP
258 fluorescence intensity in *prmt5* morphants as compared to control embryos (Fig. 5B-D, I-J).
259 Collectively, these data indicate that the transcriptional control of *cdh5* is independent of Prmt5
260 methyltransferase activity and could rather rely on a role of Prmt5 as a scaffold protein to
261 provide a proper chromatin conformation context.
262

263 **DISCUSSION**

264 Here we have demonstrated a role for Prmt5 in both hematopoiesis and blood vessel formation
265 in zebrafish. Our results suggest that Prmt5 promotes vascular morphogenesis through the
266 transcriptional control of ETS transcription factor and adhesion proteins in endothelial cells.
267 Intriguingly, we have shown that the methyltransferase activity of Prmt5 was not absolutely
268 required to regulate gene expression, leading us to propose a role of scaffold protein for Prmt5
269 to facilitate chromatin looping formation in endothelial cells.

270 We found that, similarly as in mouse (Liu et al., 2015a), Prmt5 plays an important role in
271 zebrafish hematopoiesis by controlling HSCs emergence and HSPCs expansion. We also
272 described for the first time the involvement of Prmt5 in vascular morphogenesis by regulating
273 the expression of known genes that control this process (adhesion proteins or transcription
274 factors). Actually, *prmt5* loss of function partially phenocopied loss of function of these genes.
275 Indeed, it was shown that knocking down individual ETS proteins had limited effect on sprout
276 formation, while the combination of morpholinos against both *fli1a, fli1b,* and *ets1* led to a
277 decreased number of vessel sprouts at 24 hpf but to a normal trunk vasculature at 48 hpf
278 (Pham et al., 2007). Moreover, *amolt2a* knock down in zebrafish led to a reduced diameter of
279 the DA in a similar way as we found in the context of *prmt5* loss of function (Hultin et al., 2014).
280 Furthermore, disconnected stalk and tip cells and delayed formation of the DLAV formation
281 that we observed in *prmt5* mutant phenocopies loss of function of both *cdh5* and *esama*
282 published in previous studies (Sauteur et al., 2017; Sauteur et al., 2014). However, the loss of
283 function of *cdh5* had no effect on HSCs emergence or HSPCs expansion (Anderson et al.,
284 2015), suggesting that Prmt5 might act on different set of genes in endothelial cells and in
285 emerging HSCs. In agreement with this hypothesis, Tan et al. have proposed that Prmt5 is
286 playing a critical role in HSC quiescence through the splicing of genes involved in DNA repair
287 (Tan et al., 2019). Of note, this study showed that Prmt5 methyltransferase activity was
288 required for controlling HSC quiescence, in agreement with our findings in the present work.
289 In contrast, our data suggest that the methyltransferase activity of Prmt5 is dispensable in

290 endothelial cells, reinforcing the idea that Prmt5 regulates transcription by different
291 mechanisms in these two processes (Fig. 6).

292 Prmt5 has been shown to facilitate ATP-dependent chromatin remodeling to promote gene
293 expression in skeletal muscles and during adipocyte differentiation (Dacwag et al., 2009;
294 LeBlanc et al., 2012; LeBlanc et al., 2016; Pal et al., 2003). Here, we propose that Prmt5 could
295 also be essential for proper chromatin looping in endothelial cells. Our data suggest that Prmt5
296 influences gene expression only in an endogenous context where chromatin looping is
297 required (*e.g. chd5* and *TgBAC(cdh5:GAL4FF))*, while it is dispensable for gene expression
298 when enhancer and promotor regions are artificially associated (*e.g. Tg(cdh5:Gal4VP16))* or
299 close by (*e.g. fli1a*). This implies that Prmt5 could interact with Brg1 ATPase of SWI/SNF
300 chromatin remodeling complex and with the Mediator complex in endothelial cells as it does in
301 muscle cells and adipocytes. Consistent with this hypothesis, *brg1* mutant mouse embryos
302 display an anemia coupled to vascular defects in the yolk sac, characterized by thin vessels
303 and supernumerary sprouts (Griffin et al., 2008), which is reminiscent to our present findings
304 in zebrafish *prmt5* mutant. Interestingly, it has been proposed that the mediator complex
305 regulates endothelial cell differentiation (Napoli et al., 2019). Moreover, our analyses of the
306 published single cell expression data (Wagner et al., 2018) indicate that, similarly to *prmt5*, the
307 expression of *smarc4a/brg1* and *med12* in zebrafish endothelial cells is detected as early as
308 10 hpf and decreases in subsequent stages. It is thus tempting to speculate that Prmt5, Brg1
309 and the Mediator could act together to regulate chromatin organization in endothelial cells (Fig.
310 6).

311 ChIP-seq data available in mouse revealed that some flanking regions of orthologues of
312 identified Prmt5 target genes are bound by ETV2 and present histone marks associated with
313 the recruitment of Prmt5. In zebrafish, both *prmt5* and *etv2* genes are expressed at early stage
314 in endothelial cells, and Etv2 binding motif is enriched in *cis*-regulatory regions identified by
315 ATAC-seq experiment (Quillien et al., 2017). In addition, zebrafish mutant for *prmt5* from our
316 study and a mutant for the master regulator *etv2* shared similarities in their phenotypes

317 displaying abnormal vasculature at 48 hpf characterized by a lack of lumen formation, a lack
318 of vessel extension and aberrant connections (Craig et al., 2015; Pham et al., 2007). Here, we
319 proposed that Etv2 could be involved in the recruitments of Prmt5 to *cis* regulatory regions of
320 endothelial genes. Another crucial player of blood vessel formation is the transcription factor
321 Npas4l, which is expressed during late gastrulation and regulates *etv2* expression (Marass et
322 al., 2019). Npas4l ChIP-seq data and ATAC-seq data from *npas4l* mutant also revealed the
323 binding of this transcription factor to a certain number of cis-regulatory regions of Prmt5 target
324 genes identified in the present work. In light of these findings, we speculate that Npas4l could
325 contribute to the recruitment of Prmt5 to endothelial genes (AQ and LV, unpublished data).
326 Even though technically highly challenging at the present time, ChIP-seq against Prmt5 or any
327 known Prmt5 substrates in endothelial cells in zebrafish combined with the corresponding
328 RNA-seq/ATAC-seq experiments in wild type or mutant condition for Prmt5 could help to
329 validate our model and identify all Prmt5 putative target genes.

330 The presence of Prmt5 and Brg1 at promotor regions of the *PPARγ2* locus or of *myogenin* was
331 associated with dimethylated H3R8 (histone 3 arginine 8) (Dacwag et al., 2009; LeBlanc et al.,
332 2012). Interestingly, *prmt5* knock down led to a reduction of both histone methylation and
333 chromatin looping formation (Dacwag et al., 2009; LeBlanc et al., 2012; LeBlanc et al., 2016).
334 *In vitro*, the addition of Prmt5 to Brg1-immunopurified complexes enhanced histone
335 methylation, while the addition of a catalytic dead version of Prmt5 did not (Pal et al., 2003).
336 Altogether these data suggest that wild type Prmt5, when recruited to target gene promoter
337 regions, acts most likely by dimethylating histone proteins. However, these studies did not
338 assess the ability of Prmt5 to facilitate chromatin looping independently (or not) of its
339 methyltransferase activity. Our data suggest that chromatin looping favored by Prmt5 does not
340 necessarily require its methyltransferase activity. Indeed, rescue experiments demonstrated
341 that Prmt5 was able to restore gene expression independently of its enzymatic activity, with
342 the exception of *fli1a* expression. Since *fli1a* putative enhancer is located only at 700 pb from
343 the promoter region, chromatin looping might not be required for *fli1a* expression and Prmt5

344 might essentially act here through its methyltransferase activity. Hence, depending on the
345 context and the target genes considered, Prmt5 could modulate gene expression in endothelial
346 cell through promotion of chromatin interaction and/or *via* histones/proteins modification.
347 Finally, we can consider that other proteins of the PRMT family could also regulate endothelial
348 gene expression, as some PRMT members are also expressed in zebrafish endothelial cells
349 (AQ and LV, unpublished data). For instance, ChIP-seq data in chicken erythrocytes suggest
350 that both Prmt5 and Prmt1 are recruited to the same cis-regulatory regions with Prmt1
351 permitting the recruitments of CBP/p300 to acetylate histones (Beacon et al., 2020). Hence,
352 analyses of the role(s) of other PRMT family members in endothelial cells would help to better
353 understand the cross-talks between these enzymes. Besides their function during normal
354 development, it has been shown in a zebrafish xenotransplantation model that Etv2 and Fli1b
355 are required for tumor angiogenesis, suggesting that inhibition of these ETS factors may
356 present a novel strategy to inhibit tumor angiogenesis and reduce tumor growth (Baltrunaite et
357 al., 2017). We found that Prmt5 activates ETV2 target gene expression, and Prmt5 has been
358 proposed as a therapeutic target in many diseases, including cancer (Shailesh et al., 2018).
359 Several Prmt5 inhibitors have been discovered in the past decade and some have been tested
360 in clinical trials for the treatment of tumors (reviewed in (Wang et al., 2018)). However, the vast
361 majority, if not all, compounds discovered and validated so far inhibit Prmt5 enzymatic activity
362 (Lin and Luengo, 2019). Yet, we show here that Prmt5 acts at least in part, independently of
363 its methyltransferase activity to regulate vascular morphogenesis. Hence, our data shed light
364 on a mechanism of action of Prmt5 that will be insensitive to the afore mentioned enzymatic
365 inhibitors and thus calls forth the design of alternative drugs *i.e*. specific inhibitors of the
366 interaction between Prmt5 and Etv2 in this context. In conclusion, our study highlights different
367 modes of regulation of gene expression by Prmt5 in endothelial cells and strengthens the
368 importance of its enzymatic-independent function in chromatin looping. This non-canonical
369 function of Prmt5 may have a more pervasive role than previously thought in physiological
370 conditions *i.e.* during development but also in pathological situations such as in tumor
371 angiogenesis and this aspect certainly deserves more attention in the future.

372

373 **MATERIALS AND METHODS**

374 **Zebrafish care and maintenance**

375 Embryos were raised and staged according to standard protocols and the Recommended
376 Guidelines for Zebrafish Husbandry Conditions (Alestrom et al., 2019; Kimmel et al., 1995).
377 The establishment and characterization of Tg(gata2b:Gal4;UAS:lifeactGFP), Tg(fli1a:eGFP),
378 Tg(TP1bglob:VenusPEST)s940, TgBAC(cdh5:GAL4FF);Tg(UAS:GFP), Tg(UAS:KAEDE)
379 have been described elsewhere (Bussmann and Schulte-Merker, 2011; Butko et al., 2015;
380 Hatta et al., 2006; Lawson and Weinstein, 2002b; Ninov et al., 2012). Lines generated in this
381 study are described below. Embryos were fixed overnight at 4°C in BT-FIX, after which they
382 were immediately processed or dehydrated and stored at −20°C until use.

383 **Ethics statement**

384 Fish were handled in a facility certified by the French Ministry of Agriculture (approval number
385 A3155510). The project has received an agreement number APAFIS#7124-20161
386 00517263944 v3. Anesthesia and euthanasia procedures were performed in Tricaine
387 Methanesulfonate (MS222) solutions as recommended for zebrafish (0.16 mg/ml for
388 anesthesia, 0.30 mg/ml for euthanasia). All efforts were made to minimize the number of
389 animals used and their suffering, in accordance with the guidelines from the European directive
390 on the protection of animals used for scientific purposes (2010/63/UE) and the guiding
391 principles from the French Decret 2013–118.

392 **Plasmid construction**

393 To construct the transgene Tg(*cdh5:GAL4VP16*), we cloned the putative *cdh5* promoter
394 (*cdh5*P) and enhancer (*cdh5*E) elements into pme_mcs and p5E_GGWDest+ (Addgene
395 #49319) (Kirchmaier et al., 2013; Kwan et al., 2007) using XhoI, EcoRI and BsaI to give
396 pme_*cdh5*P and p5E_*cdh5*E, respectively. The Gal4VP16 sequence from pme_Gal4VP16

397 (Kwan et al., 2007) was then introduced downstream of *cdh5*P into pme_*cdh5*P using BamH1
398 and SpeI. A multisite LR recombination reaction (Gateway LR Clonase II Enzyme mix,
399 Invitrogen) was then performed using p5E_*cdh5*E, pme_*cdh5*P:Gal4VP16, with pminTol-R4-
400 R2pA to give pminTol- *cdh5*E-*cdh5*P: Gal4VP16. Oligonucleotide sequences are listed in
401 Table S2.

402 **Generation of *prmt5*$^{-/-}$ mutants by CRISPR/cas9**

403 The guide RNA (gRNA) was designed using CHOPCHOP CRISPR Design website (Montague
404 et al., 2014). The designed oligos were annealed and ligated into the gRNA plasmid pDR274
405 after digestion of the plasmid with BsaI (NEB). The gRNA was prepared *in vitro* using the
406 MEGAshortscript T7 transcription kit (Ambion) after linearizing the plasmid with DraI (NEB)
407 (Talbot and Amacher, 2014) before being purified using illustra MicroSpin G-50 Columns (GE
408 Healthcare). 1 nL of a solution containing 10µM EnGen Cas9 NLS (NEB) and 100 ng/µl of
409 gRNA was injected at the one-cell stage. WT, heterozygous, and homozygous *prmt5* animals
410 were identified by PCR. Oligonucleotide sequences are listed in Table S2.

411 **Microinjections**

412 The Tg(*cdh5:GAL4VP16*);Tg(*UAS:KAEDE*) line was generated using pminTol- *cdh5*E-*cdh5*P:
413 Gal4VP16 by Tol2 transposition as described previously (Covassin et al., 2009). Control and
414 *prmt5* morpholino oligonucleotides (MOs) were described previously (Batut et al., 2011).
415 Embryos from in-crosses of the indicated heterozygous carriers or wild-type adults were
416 injected at the one cell stage with 6 ng of MO. pBluescript II KS+ hPRMT5 WT and pBluescript
417 II KS+ hPRMT5 Mutant (Pal et al., 2003) were linearized by EcoRI (NEB) and transcribed by
418 T7 (Promega). 200 pg *hprmt5WT* mRNA, or *hprmt5 MUT* mRNA were injected at one cell
419 stage.

420 **RNA extraction, Reverse transcription and real-time PCR**

421 Embryos were dissected at the indicated stage after addition of Tricaine Methanesulfonate.
422 Genomic DNA was extracted from dissected embryo heads to identify their genotype and the

423 corresponding dissected tails were conserved in TRIzol Reagent at -20°C. After identification
424 of wild type and mutant embryos, total RNAs from at least 6 identified tails were extracted
425 following manufacturer's instructions (Invitrogen). Total RNAs were converted into cDNA using
426 Prime Script cDNA Synthesis Kit (Takara) with Oligo(dT) and random hexamer primers for
427 15 min at 37 °C according to manufacturer's instructions. cDNAs were then diluted 20-fold and
428 quantified by qPCR using SsoFast Evagreen Supermix (Bio-rad) and specific primers. Data
429 were acquired on CFX96 Real-Time PCR detection System (Bio-rad). Samples were analyzed
430 in triplicates and the expression level was calculated relative to zebrafish housekeeping gene
431 *EF1α*. Oligonucleotide sequences are listed in Table S2.

432 **Live imaging**

433 For the transgenic lines *TgBAC(cdh5:GAL4FF);*Tg(*UAS:GFP*) and
434 Tg(*cdh5:GAL4VP16*);Tg(*UAS:KAEDE*), embryos were placed in 1.5% low melt agarose with
435 Tricaine on a glass-bottomed culture dish filled with egg water. Images were acquired using
436 the confocal microscope TCS SP8 (Leica Microsystems) with an L 25 × /0.95 W FLUOSTAR
437 VIZIR objective (zoom X1.25) using the scanner resonant mode. Confocal stacks were
438 acquired every 10 min from 28 to 38 hpf to generate movies.

439 **Immunostaining and *in situ* hybridization**

440 After fixation or rehydratation, embryos were washed twice with Phosphate Buffered Saline/1%
441 Triton X-100 (PBST), permeabilized with PBST/0.5% Trypsin for 30 sec and washed twice
442 again with PBST. After blocking with PBST/10% Fetal Calf Serum (FCS)/1% bovine serum
443 albumin (BSA) (hereafter termed 'blocking solution') for at least 1 h, embryos were incubated
444 with antibodies directed against either GFP (Torrey Pine, Biolabs), or Prmt5 (Upstate #07405),
445 in blocking solution overnight at 4 °C followed by 5 washing steps with PBST. Embryos were
446 then incubated with the appropriate Alexa Fluor-conjugated secondary antibodies (Molecular
447 Probes) for at least 2 h at room temperature and washed three times. Nuclei were then stained
448 with TO-PRO3 (Molecular Probes) and washed twice with PBST. Embryos were dissected,

449 flat-mounted in glycerol and images were recorded on a confocal microscope as above.
450 Fluorescent *in situ* hybridization was carried out as previously described (Quillien et al., 2014).

451 **Image processing and measurements**

452 Confocal images and stacks were either analyzed with ImageJ software or LAS X. Nuclei of
453 ISV cells and gata2b+ cells were counted using the Multipoint tool of ImageJ. ISV lengths were
454 measured by drawing a line between the base and the tip of ISV on ImageJ. Contours of the
455 Dorsal Aorta were drawn using the Freehand Selection Tool with a digital pen and the area
456 was then measured. Fluorescence intensity corresponded to the measurement of average
457 gray value for each entire image.

458 **Statistical analysis**

459 Statistical comparisons of datasets were performed using GraphPad Prism software. For each
460 dataset, we tested the assumption of normality with D'Agostino-Pearson tests and accordingly,
461 unpaired t-test, Mann-Whitney test, One-way ANOVA, two-way ANOVA or Kruskal-Wallis test
462 were used to compare dataset; means (± SEM) are indicated as horizontal bars on dot plots.
463 The test used as well as the number of independent experiments performed and the minimal
464 number of biological replicates are indicated in each figure legend.

465 **Bioinformatic analysis**

466 Published single cell data from total embryos at 10hpf, 14hpf, 18hpf and 24hpf (Wagner et al.,
467 2018) were analyzed using the R package Seurat (Butler et al., 2018; Stuart et al., 2019). After
468 data clustering, clusters of endothelial cells from each stage were identified by the expression
469 of several endothelial specific genes (*etv2*, *fli1a*, …). Then, we examined the level of
470 expression and the percentage of cells expressing our gene of interest at each developmental
471 stage. ATAC-seq data (Marass et al., 2019; Quillien et al., 2017) and Chip-seq data (Girardot
472 et al., 2014; Liu et al., 2015a) were inspected using the Galaxy platform (Afgan et al., 2018).

473

474 **ACKNOWLEDGEMENTS**

475 We would like to thank the Blader lab for helpful discussions and support; Dr. Waltzer, Dr. Cau,
476 Dr. Male and Dr. Navajas Acedo for critical reading of the manuscript; A. Laire for excellent
477 zebrafish care; B. Ronsin and S. Bosch from the Toulouse Rio Imaging (TRI) platform; M.
478 Aguirrebengoa from the BigA Core Facility, CBI Toulouse; Dr. Herbomel for the Zebrafish
479 transgenic line *Tg(gata2b:Gal4;UAS:lifeactGFP).* This work was supported by a grant from the
480 Fondation de l'Association pour la Recherche contre le Cancer (Fondation ARC) and from the
481 Association Française contre les Myopathies (AFM) to LV. AQ was supported by a fellowship
482 from the Fondation ARC.

483

484 **COMPETING INTEREST**

485 The authors declare no competing interests.

486

487 **REFERENCES**

488 Afgan, E., Baker, D., Batut, B., van den Beek, M., Bouvier, D., Cech, M., Chilton, J., Clements,
489 D., Coraor, N., Gruning, B.A.*, et al.* (2018). The Galaxy platform for accessible, reproducible
490 and collaborative biomedical analyses: 2018 update. Nucleic Acids Res *46*, W537-W544.
491 Alestrom, P., D'Angelo, L., Midtlyng, P.J., Schorderet, D.F., Schulte-Merker, S., Sohm, F., and
492 Warner, S. (2019). Zebrafish: Housing and husbandry recommendations. Lab Anim,
493 23677219869037.
494 Anderson, H., Patch, T.C., Reddy, P.N., Hagedorn, E.J., Kim, P.G., Soltis, K.A., Chen, M.J.,
495 Tamplin, O.J., Frye, M., MacLean, G.A.*, et al.* (2015). Hematopoietic stem cells develop in the
496 absence of endothelial cadherin 5 expression. Blood *126*, 2811-2820.
497 Baltrunaite, K., Craig, M.P., Palencia Desai, S., Chaturvedi, P., Pandey, R.N., Hegde, R.S.,
498 and Sumanas, S. (2017). ETS transcription factors Etv2 and Fli1b are required for tumor
499 angiogenesis. Angiogenesis *20*, 307-323.
500 Batut, J., Duboe, C., and Vandel, L. (2011). The methyltransferases PRMT4/CARM1 and
501 PRMT5 control differentially myogenesis in zebrafish. PLoS One *6*, e25427.

502 Beacon, T.H., Xu, W., and Davie, J.R. (2020). Genomic landscape of transcriptionally active
503 histone arginine methylation marks, H3R2me2s and H4R3me2a, relative to nucleosome
504 depleted regions. Gene *742*, 144593.
505 Beis, D., and Stainier, D.Y. (2006). In vivo cell biology: following the zebrafish trend. Trends
506 Cell Biol *16*, 105-112.
507 Blanc, R.S., and Richard, S. (2017). Arginine Methylation: The Coming of Age. Mol Cell *65*, 8-
508 24.
509 Bussmann, J., and Schulte-Merker, S. (2011). Rapid BAC selection for tol2-mediated
510 transgenesis in zebrafish. Development *138*, 4327-4332.
511 Butko, E., Distel, M., Pouget, C., Weijts, B., Kobayashi, I., Ng, K., Mosimann, C., Poulain, F.E.,
512 McPherson, A., Ni, C.W.*, et al.* (2015). Gata2b is a restricted early regulator of hemogenic
513 endothelium in the zebrafish embryo. Development *142*, 1050-1061.
514 Butler, A., Hoffman, P., Smibert, P., Papalexi, E., and Satija, R. (2018). Integrating single-cell
515 transcriptomic data across different conditions, technologies, and species. Nat Biotechnol *36*,
516 411-420.
517 Covassin, L.D., Siekmann, A.F., Kacergis, M.C., Laver, E., Moore, J.C., Villefranc, J.A.,
518 Weinstein, B.M., and Lawson, N.D. (2009). A genetic screen for vascular mutants in zebrafish
519 reveals dynamic roles for Vegf/Plcg1 signaling during artery development. Dev Biol *329*, 212-
520 226.
521 Craig, M.P., Grajevskaja, V., Liao, H.K., Balciuniene, J., Ekker, S.C., Park, J.S., Essner, J.J.,
522 Balciunas, D., and Sumanas, S. (2015). Etv2 and fli1b function together as key regulators of
523 vasculogenesis and angiogenesis. Arterioscler Thromb Vasc Biol *35*, 865-876.
524 Dacwag, C.S., Bedford, M.T., Sif, S., and Imbalzano, A.N. (2009). Distinct protein arginine
525 methyltransferases promote ATP-dependent chromatin remodeling function at different stages
526 of skeletal muscle differentiation. Mol Cell Biol *29*, 1909-1921.
527 Fish, J.E., Cantu Gutierrez, M., Dang, L.T., Khyzha, N., Chen, Z., Veitch, S., Cheng, H.S.,
528 Khor, M., Antounians, L., Njock, M.S.*, et al.* (2017). Dynamic regulation of VEGF-inducible
529 genes by an ERK/ERG/p300 transcriptional network. Development *144*, 2428-2444.
530 Girardot, M., Hirasawa, R., Kacem, S., Fritsch, L., Pontis, J., Kota, S.K., Filipponi, D., Fabbrizio,
531 E., Sardet, C., Lohmann, F.*, et al.* (2014). PRMT5-mediated histone H4 arginine-3 symmetrical
532 dimethylation marks chromatin at G + C-rich regions of the mouse genome. Nucleic Acids Res
533 *42*, 235-248.
534 Griffin, C.T., Brennan, J., and Magnuson, T. (2008). The chromatin-remodeling enzyme BRG1
535 plays an essential role in primitive erythropoiesis and vascular development. Development
536 *135*, 493-500.
537 Hatta, K., Tsujii, H., and Omura, T. (2006). Cell tracking using a photoconvertible fluorescent
538 protein. Nat Protoc *1*, 960-967.

539 Hultin, S., Zheng, Y., Mojallal, M., Vertuani, S., Gentili, C., Balland, M., Milloud, R., Belting,
540 H.G., Affolter, M., Helker, C.S.*, et al.* (2014). AmotL2 links VE-cadherin to contractile actin
541 fibres necessary for aortic lumen expansion. Nat Commun *5*, 3743.
542 Isogai, S., Horiguchi, M., and Weinstein, B.M. (2001). The vascular anatomy of the developing
543 zebrafish: an atlas of embryonic and early larval development. Dev Biol *230*, 278-301.
544 Kalna, V., Yang, Y., Peghaire, C.R., Frudd, K., Hannah, R., Shah, A.V., Osuna Almagro, L.,
545 Boyle, J.J., Gottgens, B., Ferrer, J.*, et al.* (2019). The Transcription Factor ERG Regulates
546 Super-Enhancers Associated With an Endothelial-Specific Gene Expression Program. Circ
547 Res *124*, 1337-1349.
548 Karkhanis, V., Hu, Y.J., Baiocchi, R.A., Imbalzano, A.N., and Sif, S. (2011). Versatility of
549 PRMT5-induced methylation in growth control and development. Trends Biochem Sci *36*, 633-
550 641.
551 Kimmel, C.B., Ballard, W.W., Kimmel, S.R., Ullmann, B., and Schilling, T.F. (1995). Stages of
552 embryonic development of the zebrafish. Dev Dyn *203*, 253-310.
553 Kirchmaier, S., Lust, K., and Wittbrodt, J. (2013). Golden GATEway cloning--a combinatorial
554 approach to generate fusion and recombination constructs. PLoS One *8*, e76117.
555 Kwan, K.M., Fujimoto, E., Grabher, C., Mangum, B.D., Hardy, M.E., Campbell, D.S., Parant,
556 J.M., Yost, H.J., Kanki, J.P., and Chien, C.B. (2007). The Tol2kit: a multisite gateway-based
557 construction kit for Tol2 transposon transgenesis constructs. Dev Dyn *236*, 3088-3099.
558 Lawson, N.D., and Weinstein, B.M. (2002a). Arteries and veins: making a difference with
559 zebrafish. Nat Rev Genet *3*, 674-682.
560 Lawson, N.D., and Weinstein, B.M. (2002b). In vivo imaging of embryonic vascular
561 development using transgenic zebrafish. Dev Biol *248*, 307-318.
562 LeBlanc, S.E., Konda, S., Wu, Q., Hu, Y.J., Oslowski, C.M., Sif, S., and Imbalzano, A.N.
563 (2012). Protein arginine methyltransferase 5 (Prmt5) promotes gene expression of peroxisome
564 proliferator-activated receptor gamma2 (PPARgamma2) and its target genes during
565 adipogenesis. Mol Endocrinol *26*, 583-597.
566 LeBlanc, S.E., Wu, Q., Lamba, P., Sif, S., and Imbalzano, A.N. (2016). Promoter-enhancer
567 looping at the PPARgamma2 locus during adipogenic differentiation requires the Prmt5
568 methyltransferase. Nucleic Acids Res *44*, 5133-5147.
569 Lin, H., and Luengo, J.I. (2019). Nucleoside protein arginine methyltransferase 5 (PRMT5)
570 inhibitors. Bioorg Med Chem Lett *29*, 1264-1269.
571 Liu, F., Cheng, G., Hamard, P.J., Greenblatt, S., Wang, L., Man, N., Perna, F., Xu, H., Tadi,
572 M., Luciani, L.*, et al.* (2015a). Arginine methyltransferase PRMT5 is essential for sustaining
573 normal adult hematopoiesis. J Clin Invest *125*, 3532-3544.

574 Liu, F., Li, D., Yu, Y.Y., Kang, I., Cha, M.J., Kim, J.Y., Park, C., Watson, D.K., Wang, T., and
575 Choi, K. (2015b). Induction of hematopoietic and endothelial cell program orchestrated by ETS
576 transcription factor ER71/ETV2. EMBO Rep *16*, 654-669.
577 Ma, D., Wei, Y., and Liu, F. (2013). Regulatory mechanisms of thymus and T cell development.
578 Dev Comp Immunol *39*, 91-102.
579 Marass, M., Beisaw, A., Gerri, C., Luzzani, F., Fukuda, N., Gunther, S., Kuenne, C.,
580 Reischauer, S., and Stainier, D.Y.R. (2019). Genome-wide strategies reveal target genes of
581 Npas4l associated with vascular development in zebrafish. Development *146*.
582 Montague, T.G., Cruz, J.M., Gagnon, J.A., Church, G.M., and Valen, E. (2014). CHOPCHOP:
583 a CRISPR/Cas9 and TALEN web tool for genome editing. Nucleic Acids Res *42*, W401-407.
584 Napoli, C., Schiano, C., and Soricelli, A. (2019). Increasing evidence of pathogenic role of the
585 Mediator (MED) complex in the development of cardiovascular diseases. Biochimie *165*, 1-8.
586 Ninov, N., Borius, M., and Stainier, D.Y. (2012). Different levels of Notch signaling regulate
587 quiescence, renewal and differentiation in pancreatic endocrine progenitors. Development
588 *139*, 1557-1567.
589 Pal, S., Yun, R., Datta, A., Lacomis, L., Erdjument-Bromage, H., Kumar, J., Tempst, P., and
590 Sif, S. (2003). mSin3A/histone deacetylase 2- and PRMT5-containing Brg1 complex is
591 involved in transcriptional repression of the Myc target gene cad. Mol Cell Biol *23*, 7475-7487.
592 Pham, V.N., Lawson, N.D., Mugford, J.W., Dye, L., Castranova, D., Lo, B., and Weinstein,
593 B.M. (2007). Combinatorial function of ETS transcription factors in the developing vasculature.
594 Dev Biol *303*, 772-783.
595 Quillien, A., Abdalla, M., Yu, J., Ou, J., Zhu, L.J., and Lawson, N.D. (2017). Robust
596 Identification of Developmentally Active Endothelial Enhancers in Zebrafish Using FANS-
597 Assisted ATAC-Seq. Cell Rep *20*, 709-720.
598 Quillien, A., Moore, J.C., Shin, M., Siekmann, A.F., Smith, T., Pan, L., Moens, C.B., Parsons,
599 M.J., and Lawson, N.D. (2014). Distinct Notch signaling outputs pattern the developing arterial
600 system. Development *141*, 1544-1552.
601 Rosa-Garrido, M., Chapski, D.J., and Vondriska, T.M. (2018). Epigenomes in Cardiovascular
602 Disease. Circ Res *122*, 1586-1607.
603 Sauteur, L., Affolter, M., and Belting, H.G. (2017). Distinct and redundant functions of Esama
604 and VE-cadherin during vascular morphogenesis. Development *144*, 1554-1565.
605 Sauteur, L., Krudewig, A., Herwig, L., Ehrenfeuchter, N., Lenard, A., Affolter, M., and Belting,
606 H.G. (2014). Cdh5/VE-cadherin promotes endothelial cell interface elongation via cortical actin
607 polymerization during angiogenic sprouting. Cell Rep *9*, 504-513.
608 Shailesh, H., Zakaria, Z.Z., Baiocchi, R., and Sif, S. (2018). Protein arginine methyltransferase
609 5 (PRMT5) dysregulation in cancer. Oncotarget *9*, 36705-36718.

610 Stopa, N., Krebs, J.E., and Shechter, D. (2015). The PRMT5 arginine methyltransferase: many
611 roles in development, cancer and beyond. Cell Mol Life Sci *72*, 2041-2059.
612 Stuart, T., Butler, A., Hoffman, P., Hafemeister, C., Papalexi, E., Mauck, W.M., 3rd, Hao, Y.,
613 Stoeckius, M., Smibert, P., and Satija, R. (2019). Comprehensive Integration of Single-Cell
614 Data. Cell *177*, 1888-1902 e1821.
615 Talbot, J.C., and Amacher, S.L. (2014). A streamlined CRISPR pipeline to reliably generate
616 zebrafish frameshifting alleles. Zebrafish *11*, 583-585.
617 Tan, D.Q., Li, Y., Yang, C., Li, J., Tan, S.H., Chin, D.W.L., Nakamura-Ishizu, A., Yang, H., and
618 Suda, T. (2019). PRMT5 Modulates Splicing for Genome Integrity and Preserves Proteostasis
619 of Hematopoietic Stem Cells. Cell Rep *26*, 2316-2328 e2316.
620 Tee, W.W., Pardo, M., Theunissen, T.W., Yu, L., Choudhary, J.S., Hajkova, P., and Surani,
621 M.A. (2010). Prmt5 is essential for early mouse development and acts in the cytoplasm to
622 maintain ES cell pluripotency. Genes Dev *24*, 2772-2777.
623 Thisse, C., and Zon, L.I. (2002). Organogenesis--heart and blood formation from the zebrafish
624 point of view. Science *295*, 457-462.
625 Wagner, D.E., Weinreb, C., Collins, Z.M., Briggs, J.A., Megason, S.G., and Klein, A.M. (2018).
626 Single-cell mapping of gene expression landscapes and lineage in the zebrafish embryo.
627 Science *360*, 981-987.
628 Wang, Y., Hu, W., and Yuan, Y. (2018). Protein Arginine Methyltransferase 5 (PRMT5) as an
629 Anticancer Target and Its Inhibitor Discovery. J Med Chem *61*, 9429-9441.
630 Wong, K.S., Proulx, K., Rost, M.S., and Sumanas, S. (2009). Identification of vasculature-
631 specific genes by microarray analysis of Etsrp/Etv2 overexpressing zebrafish embryos. Dev
632 Dyn *238*, 1836-1850.
633 Zhu, J., Zhang, D., Liu, X., Yu, G., Cai, X., Xu, C., Rong, F., Ouyang, G., Wang, J., and Xiao,
634 W. (2019). Zebrafish prmt5 arginine methyltransferase is essential for germ cell development.
635 Development *146*.

636

637 **FIGURE LEGENDS**

638 **Figure 1: Loss of *prmt5* affect HSCs and HSPCs production. A**- Schematic representation
639 of the sequence targeted by CRISPR/Cas9 leading to a 23 nucleotides deletion, and of wild
640 type and truncated Prmt5 proteins. The catalytic domain “CAT” appears in magenta. **B**-**C**-
641 Confocal sections of immunostaining with anti-Prmt5 antibody of wild type and *prmt5* mutant
642 embryos at 24 hpf. Scale bar 100 µm. **D**- Schematic representation of vascular (green) and

643 hematopoietic (red) systems in a zebrafish larva. Circle and bracket indicate the Thymus (T)
644 and the Caudal Hematopoietic Tissue (CHT), respectively. **D'**- Close-up of the trunk
645 vasculature where HSCs emerge from the ventral wall of the dorsal aorta (DA), bud and
646 migrate. Red line represents the diameter of the dorsal aorta. Cardinal Vein (CV). **E**-**F'**-
647 Confocal section of transgenic *Tg*(*gata2b:Gal4; UAS:lifeactGFP*) embryos at 36 hpf showing
648 gata2b+ cells in red and TO-PRO-3 in black. Blue arrows indicate HSCs labelled in red in wild
649 type (**E**, **E'**) and in *prmt5* mutant (**F**, **F'**) embryos. Bar scale 100 µm. **G**- Average number of
650 HSCs enumerated per confocal stack in wild type and in *prmt5* mutant embryos at 36 hpf. Data
651 are from 3 independent experiments with at least 6 individuals per experiment and a Mann-
652 Whitney test was performed. **H**- Relative mRNA expressions determined by RT-qPCR in 36
653 hpf wild type and *prmt5* mutant embryos, from 3 independent experiments with at least 6
654 animals per condition. Two-way ANOVA was performed. **I**-**J**- Confocal sections of wild type (**I**)
655 and *prmt5* mutant (**J**) thymus from transgenic Tg(*gata2b:Gal4; UAS:lifeactGFP*) embryos at 5
656 days. Thymus are delimited by a white circle. Bar scale 100 µm. **K**- Average number of HSPCs
657 enumerated per confocal stack in wild type and *prmt5* mutant embryos at 5 days from 3
658 independent experiments with at least 5 individuals per analysis. T-test was performed. *
659 P<0.05, ** P<0.01, ***P<0.001.

660 **Figure 2: Loss of *prmt5* impairs blood vessel formation**. **A**-**C'**- Confocal projections of
661 transgenic *Tg(fli1a:GFP)*^{y1} embryos with endothelial cells (in green) after immunostaining
662 against Prmt5 (in magenta). **A**-**A''**- Dorsal view of the lateral plate mesoderm at 14 somite-
663 stage. Yellow rectangle delimits the close up of Prmt5+ endothelial cells (**A'**-**A''**). Prmt5+ cells
664 appear in magenta (**A**-**A"**) and endothelial cells in green (**A**-**A'**). Anterior is on top. Scale bars
665 100 µm (**A**) and 25 µm (**A'**). **B**-**B'**- Confocal projections focusing on endothelial cells (in green)
666 from the dorsal aorta (DA) and the cardinal vein (CV) at 24 hpf. Red and blue arrows point to
667 Prmt5+ cells (in magenta) from the DA and the CV, respectively. Red and blue lines represent
668 DA and CV diameters, respectively. Scale bar 50 µm. **C**-**C'**- Confocal projections focusing on
669 sprouting ISVs (in green) at 24 hpf. Light blue and yellow arrows point to tip and stalk cell,

670 respectively. **D**- Schematic representation of the trunk vasculature with ISVs sprouting from
671 the DA. The tip cell leads the cell migration and the stalk cell maintains the connection with the
672 DA. **E**-**F**- Confocal projections of transgenic *Tg(fli1a:GFP)*^{y1} wild type (**E**) and *prmt5* mutant (**F**)
673 embryos at 28 hpf. Red rectangles delimit where DA close ups were made. White rectangles
674 delimit the higher magnification (x2) of the DA with red lines indicating the dorsal aorta
675 diameters. White arrows indicate the connection point between two ISVs to form the Dorsal
676 Longitudinal Anastomotic Vessel (DLAV). Scale bar 100 µm. **G**-**H**- Confocal projections of
677 control morphant (**G**) and *prmt5* morphant (**H**) transgenic *Tg(TP1bglob:VenusPEST)*^{s940}
678 embryos labelling cells from the DA at 28 hpf. Yellow lines delimit the measured area occupied
679 by the DA. Scale bar 25 µm **I**- Average area occupied by the DA in μm^2 in control and *prmt5*
680 morpholino injected embryos from 2 independent experiments with at least 8 animals per
681 condition. T-test was performed. **J**-**K**- Average number of endothelial cells per intersegmental
682 vessel (**J**) and average ISV length in µm (**K**) in control and in *prmt5* mutant embryos from 3
683 independent experiments with at least 3 animals per condition. T-test and Mann Whitney test
684 were performed, respectively. ** P<0.01, ***P<0.001.

685 **Figure 3: Prmt5 is required for vascular morphogenesis. A**-**B**- Still images from movies of
686 control (**A**) and *prmt5* morphant (**B**) Tg(fli1a:GFP)^{y1} transgenic embryos from 28 to 38 hpf. Red
687 asterisks label missing connections between tip and stalk cells as well as missing connections
688 between tip cells that should lead to DLAV formation. Red arrows point to connecting ISVs
689 leading to DLAV formation. White arrows indicate supernumerary sprouts. Yellow asterisks
690 label the lumen of ISVs. Scale bar 50 µm. **C**- Relative mRNA expressions of the indicated
691 transcripts were determined by RT-qPCR in 28 hpf wild type and *prmt5* mutant embryos, from
692 3 independent experiments with at least 6 animals per condition. Two-way ANOVA was
693 performed. * P<0.05, ***P<0.001.

694 **Figure 4: Prmt5 methyltransferase activity is dispensable for vascular morphogenesis.**
695 **A**-**D**- Confocal projections of transgenic *Tg*(*fli1a:GFP*)^{y1} embryos at 28 hpf. Wild type embryo
696 is on the top left panel (**A**), *prmt5* mutant embryos were not injected (**B**) or injected with either

697 *hprmt5WT* mRNA (**C**) or the mutant form *hprmt5MUT* mRNA (**D**). Scale bar 100 µm. **E-F-**
698 Average ISVs length in µm (**E**) and average number of endothelial cells per ISVs (**F**) for wild
699 type, *prmt5* mutant embryos not injected or injected with *hprmt5WT* mRNA, or *hprmt5 MUT*
700 mRNA, from 3 independent experiments with at least 3 animals per condition. Kruskal-Wallis
701 test (**E**) and One-way ANOVA (**F**) were performed. ** P<0.01, *** P<0.001. **G**- Relative mRNA
702 expressions were determined by RT-qPCR on 28 hpf wild type and *prmt5* mutant embryos
703 injected by either *hprmt5WT or hprmt5MUT* mRNAs, from 2 independent experiments with at
704 least 6 animals per condition. Two-way ANOVA was performed. * P<0.05.

705 **Figure 5: Prmt5 promotes chromatin looping. A**- Schematic representation of the transgene
706 *TgBAC(cdh5:GAL4FF)* containing two putative cis-regulatory elements, a promotor region (P)
707 and an enhancer (E), separated by ~20kb with the *GAL4FF* reporter gene inserted at the TSS
708 of *cdh5.* **B**, **C**, **I**, **J**- Confocal projections of transgenic *TgBAC(cdh5:GAL4FF);*Tg(*UAS:GFP*)
709 embryos at 28 hpf. Control morphant is on the top left panel (**B**), *prmt5* morphant embryos
710 were not injected (**C**) or injected by either *hprmt5WT* mRNA (**I**) or the catalytic mutant form
711 *hprmt5MUT* (**J**) mRNA. The fluorescent intensity is colored-coded, from the Low intensity (L)
712 in black to High intensity (H) in white (intensity scale as in panel **B**). Scale bar 100 µm. **D-**
713 Average GFP fluorescence intensity per confocal projection for control, *prmt5* morphant
714 embryos injected by *hprmt5WT* mRNA, or *hprmt5 MUT* mRNA or not injected, from 3
715 independent experiments with at least 3 animals per condition. One-way ANOVA was
716 performed. *P<0.05, ***P<0.001. **E**- Schematic representation of the transgene
717 Tg(*cdh5:GAL4VP16*) containing the two putative cis-regulatory elements next to each other (E
718 and P), upstream of *GAL4VP16* reporter gene. **F-G-** Confocal projection of transgenic
719 Tg(*cdh5:GAL4VP16*);Tg(*UAS:KAEDE*) embryos at 26 hpf injected with either a control
720 morpholino (**F**) or *a prmt5* morpholino (**G**). The fluorescence intensity is color- coded, from the
721 Low intensity (L) in black to High intensity (H) in white (intensity scale in panel **B**). **H**- Average
722 KAEDE fluorescence intensity for control and for *prmt5* morphant embryos, from 3 independent
723 experiments with at least 5 animals per condition. T-test was performed.

724 **Figure 6: A-** Schematic representation of two distinct roles of Prmt5 during the formation of
725 hematopoietic lineage development and blood vessels, relying or not on its methyltransferase
726 activity, respectively. **B**- Proposed model to depict the function of Prmt5 in zebrafish endothelial
727 cells. The transcription factor ETV2 recruited to promoters and enhancers of endothelial
728 specific genes, could favor the recruitment of a complex including Prmt5, Brg1 and the
729 mediator complex to help the formation of chromatin loping and thus facilitate the transcription
730 of specific endothelial genes. Dashed lines indicate potential interactions or plausible
731 recruitments of Brg1 and/or the mediator complex.

732 **Figure S1: A**-**B**- Confocal sections of Prmt5 immunostaining in control and *prmt5* morphant
733 embryos at 24 hpf. Scale bar 100 µm. **C**-**F**- Confocal sections of thymus from transgenic
734 Tg(*gata2b:Gal4; UAS:lifeactGFP*) embryos at 3 days. Transgenic embryos were injected by
735 control morpholino (**C**) or *prmt5* morpholino only (**D**) or in combination *hprmt5WT* mRNA (**E**)
736 or the catalytic mutant form *hprmt5MUT* mRNA (**F**). Thymus is delimited by a white circle. Bar
737 scale 100 µm. **G**- Average number of HSPCs enumerated per confocal stack in injected
738 embryos at 3 days from 2 independent experiments with at least 3 individuals per analysis. T-
739 test was performed. ***P<0.001.

740 **Figure S2: A**-**B**- Confocal projections of transgenic Tg(*fli1a:GFP*)^{y1} embryos injected by either
741 control morpholino (**A**) or *prmt5* morpholino (**B**). Scale bar 100 µm. **C**-**D**- Average number of
742 endothelial cells per ISV (**C**) and average ISV length in µm (**D**), in control and *prmt5* morphant
743 embryos, from 3 independent experiments with at least 4 animals per condition. T-test and
744 Mann-Whitney test were performed. *** P<0.001.

745 **Figure S3**: Expression heatmap for *prmt5*, *etv2* and identified Prmt5 target genes, for
746 endothelial cells at 10hpf, 14hpf, 18hpf and 24hpf. The expression level is colored-coded from
747 absence of expression (in green) to highest level of expression (in white).

748 **Figure S4: A**-**D**- Confocal projections of wild type (**A**, **C**) and *prmt5* mutant embryos (**B**, **D**)
749 after fluorescent *in situ* hybridization against *fli1a* (**A**-**B**) and *cdh5* (**C**-**D**). Scale bar 100 µm. **E**-

750 **F-** Percentage of embryos (y axis) presenting a high or a low level of expression of *fli1a* (**E**) or
751 *cdh5* (**F**), according to their genotype (x axis), from 3 independent experiments with at least 4
752 animals per condition.

753 **Figure S5:** Chromatin profile visualization of endothelial cells from the UCSC Genome
754 Browser. ATAC-seq peaks as determined by Quillien et al. (Quillien et al., 2017) flanking
755 indicated genes (*cdh5, esama, agtr2, fli1a, fli1b, amotl2a*). Promoter regions (P) and
756 numerated putative enhancers (corresponding numerated peaks are found in Table S1) are
757 highlighted in light orange and light purple, respectively.

figure1

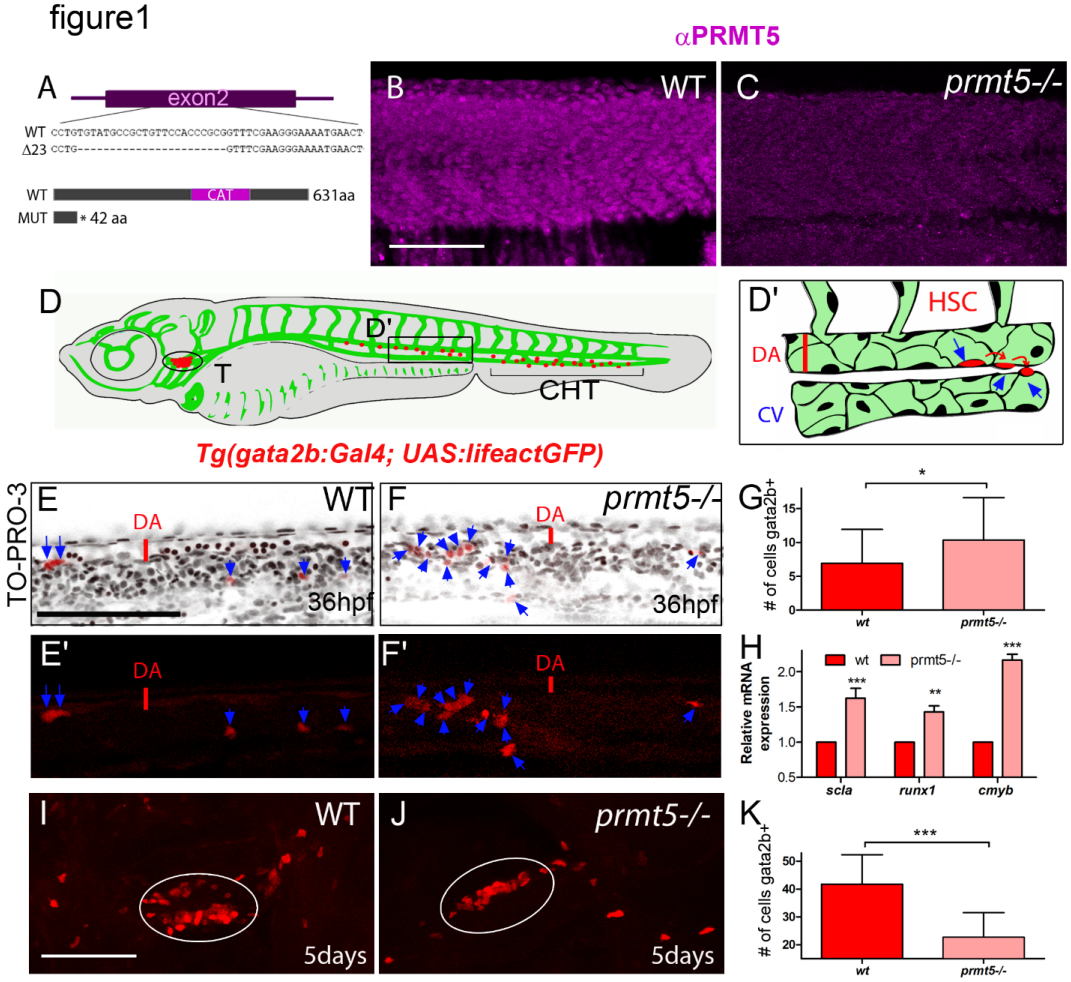
αPRMT5
A
exon2
WT CCTGTGTATGCCGCTGTTCCACCCGCGGTTTCGAAGGGAAAATGAACT
Δ23 CCTG----------GTTTCGAAGGGAAAATGAACT
WT
CAT
631aa
MUT
* 42 aa
B
WT
C
prmt5-/-
D
D'
T
CHT
D'
HSC
DA
CV
Tg(gata2b:Gal4; UAS:lifeactGFP)
TO-PRO-3
E
WT
DA
36hpf
F
prmt5-/-
DA
36hpf
G
# of cells gata2b+
wt
prmt5-/-
E'
DA
F'
DA
H
Relative mRNA expression
wt
prmt5-/-
scla
runx1
cmyb
I
WT
5days
J
prmt5-/-
5days
K
# of cells gata2b+
wt
prmt5-/-

figure2

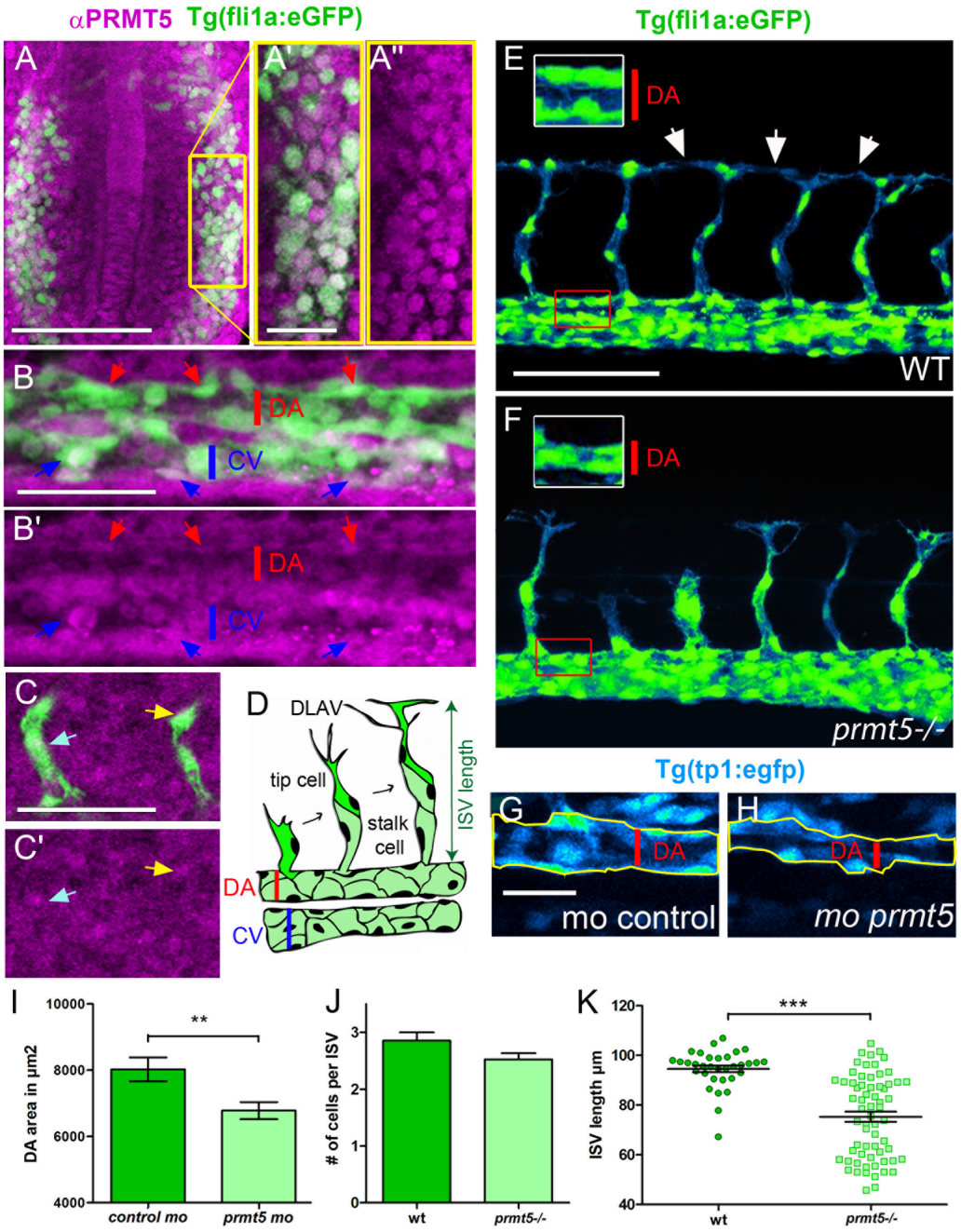
αPRMT5 Tg(fli1a:eGFP)
A
A'
A''
B
DA
CV
B'
DA
CV
C
C'
D
DLAV
tip cell
stalk cell
ISV length
DA
CV
Tg(fli1a:eGFP)
E
DA
WT
F
DA
prmt5-/-
Tg(tp1:egfp)
G
DA
mo control
H
DA
mo prmt5
I
DA area in µm2
10000
8000
6000
4000
**
control mo
prmt5 mo
J
# of cells per ISV
3
2
1
0
wt
prmt5-/-
K
ISV length µm
120
100
80
60
40
***
wt
prmt5-/-

figure3

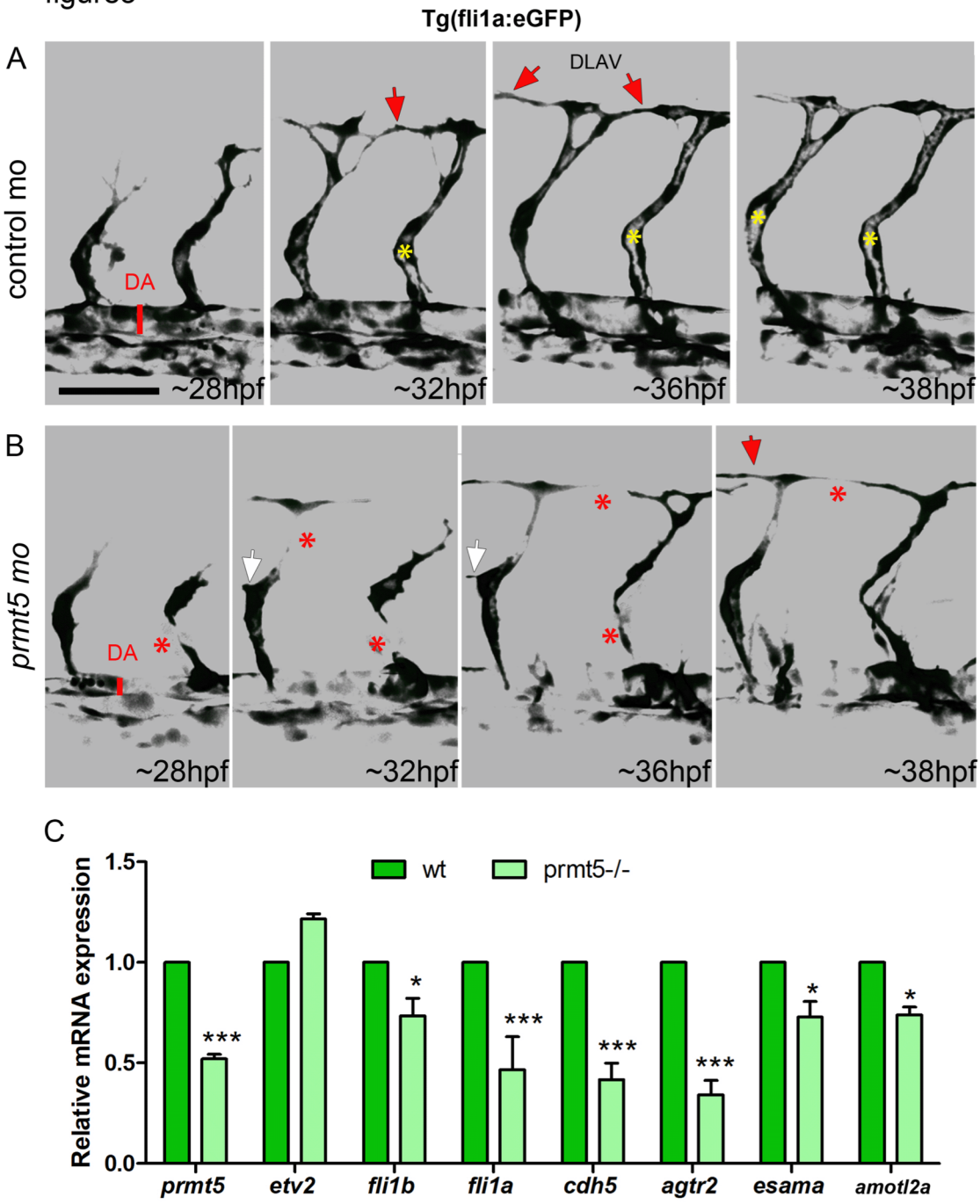
Tg(fli1a:eGFP)
A
control mo
DA
DLAV
~28hpf
~32hpf
~36hpf
~38hpf
B
prmt5 mo
DA
~28hpf
~32hpf
~36hpf
~38hpf
C
Relative mRNA expression
1.5
1.0
0.5
0.0
wt
prmt5-/-
***
*
***
***
***
*
*
prmt5
etv2
fli1b
fli1a
cdh5
agtr2
esama
amotl2a

figure4

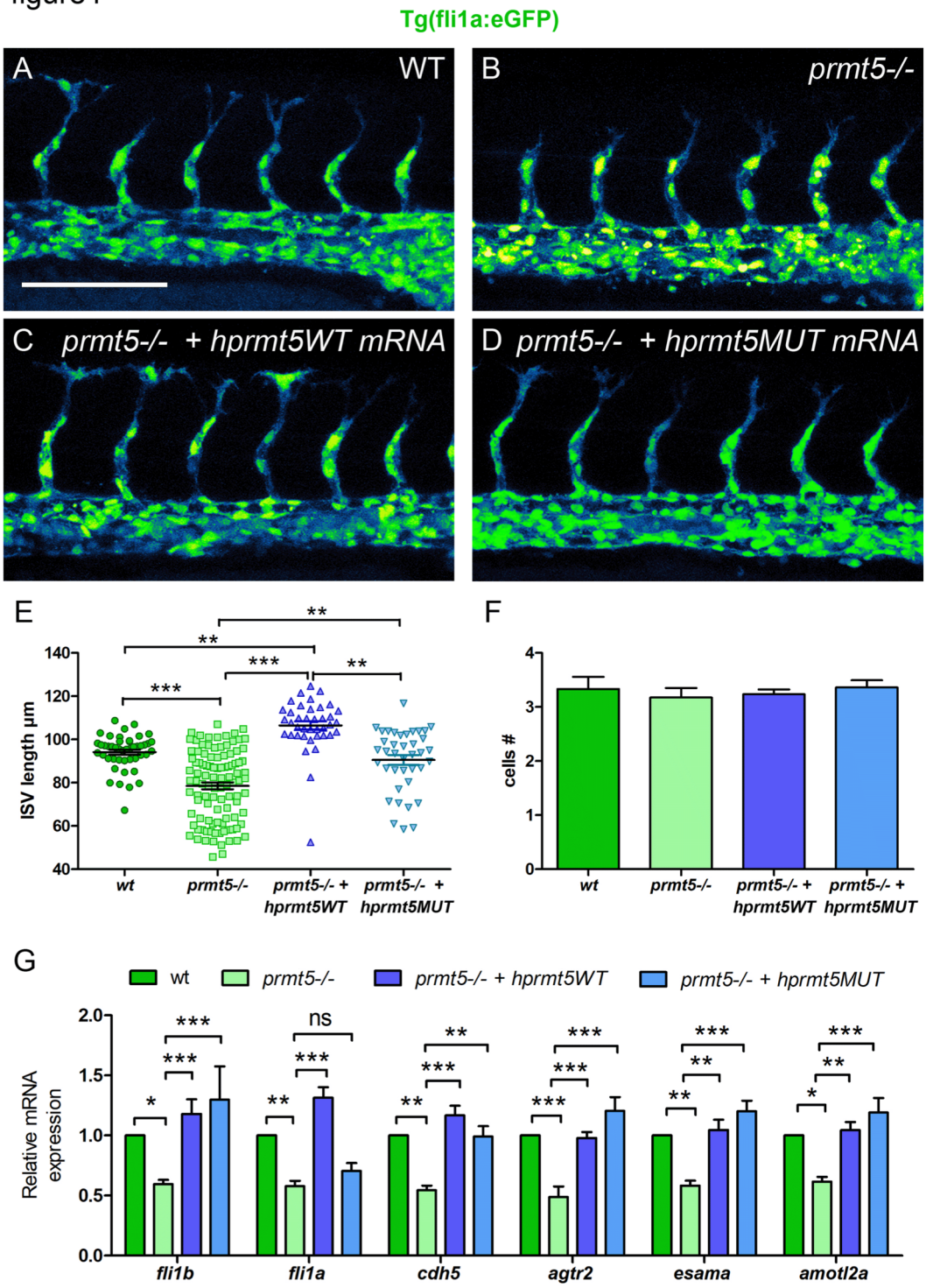
Tg(fli1a:eGFP)
A
WT
B
prmt5-/-
C
prmt5-/- + hprmt5WT mRNA
D
prmt5-/- + hprmt5MUT mRNA
E
ISV length µm
140
120
100
80
60
40
***
**
***
**
**
wt
prmt5-/-
prmt5-/- + hprmt5WT
prmt5-/- + hprmt5MUT
F
cells #
4
3
2
1
0
wt
prmt5-/-
prmt5-/- + hprmt5WT
prmt5-/- + hprmt5MUT
G
wt
prmt5-/-
prmt5-/- + hprmt5WT
prmt5-/- + hprmt5MUT
Relative mRNA expression
2.0
1.5
1.0
0.5
0.0
fli1b
fli1a
cdh5
agtr2
esama
amotl2a
ns

Gene symbol	Peak chr	Peak start	Peak stop	ETV2 CHIP Peak in mouse embryo	H4R3me2s CHIP Peak in MEF mouse cells
amotl2	*chr9*	*102,611,688*	*102,612,810*	***yes***	***yes***
amotl2	*chr9*	*102,624,400*	*102,624,850*	***yes***	*no*
cdh5	chr8	106,619,166	106,620,059	***yes***	***yes***
cdh5	chr8	106,623,076	106,623,670	***yes***	***yes***
cdh5	chr8	106,625,171	106,625,699	***yes***	***yes***
fli1	*chr9*	*32,389,460*	*32,390,252*	***yes***	*no*
fli1	*chr9*	*32,378,074*	*32,378,681*	***yes***	*no*
fli1	*chr9*	*32,363,839*	*32,364,366*	***yes***	***yes***
fli1	*chr9*	*32,348,223*	*32,349,647*	***yes***	***yes***
agtr2	chrX	_	_	*no*	***yes***

Table 1: Chromatin profile of mouse orthologous genes of prmt5 identified target genes.
List of Etv2 and H4R3me2s peaks identified by CHIP-seq in mouse embryos and in MEF mouse cells, respectively (Liu et al., 2015a; Girardot et al., 2014).

figure5

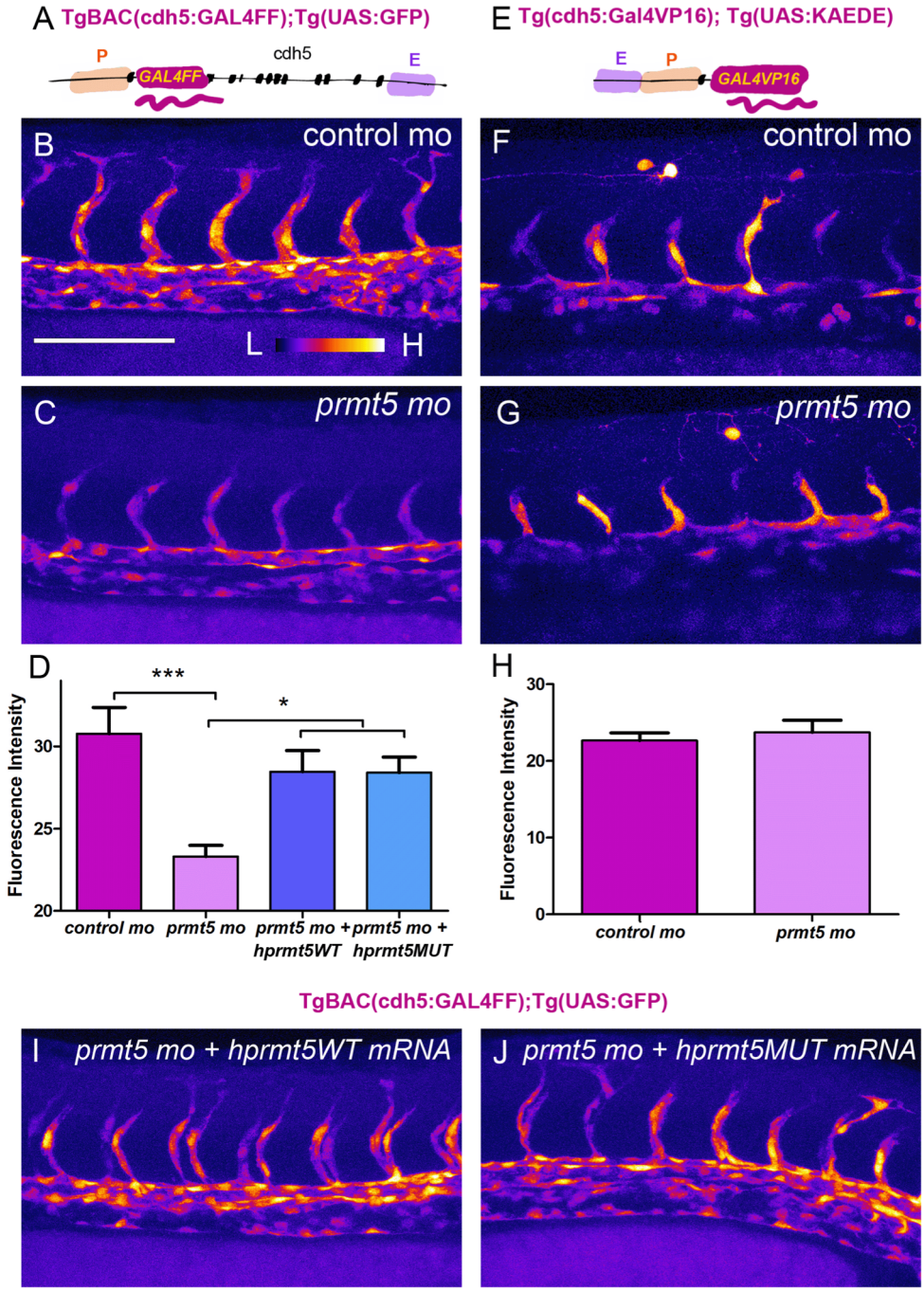
A TgBAC(cdh5:GAL4FF);Tg(UAS:GFP)
P
cdh5
E
GAL4FF
E Tg(cdh5:Gal4VP16); Tg(UAS:KAEDE)
E
P
GAL4VP16
B
control mo
L
H
F
control mo
C
prmt5 mo
G
prmt5 mo
D
***
*
Fluorescence Intensity
30
25
20
control mo
prmt5 mo
prmt5 mo + hprmt5WT
prmt5 mo + hprmt5MUT
H
Fluorescence Intensity
30
20
10
0
control mo
prmt5 mo
TgBAC(cdh5:GAL4FF);Tg(UAS:GFP)
I prmt5 mo + hprmt5WT mRNA
J prmt5 mo + hprmt5MUT mRNA

figure 6

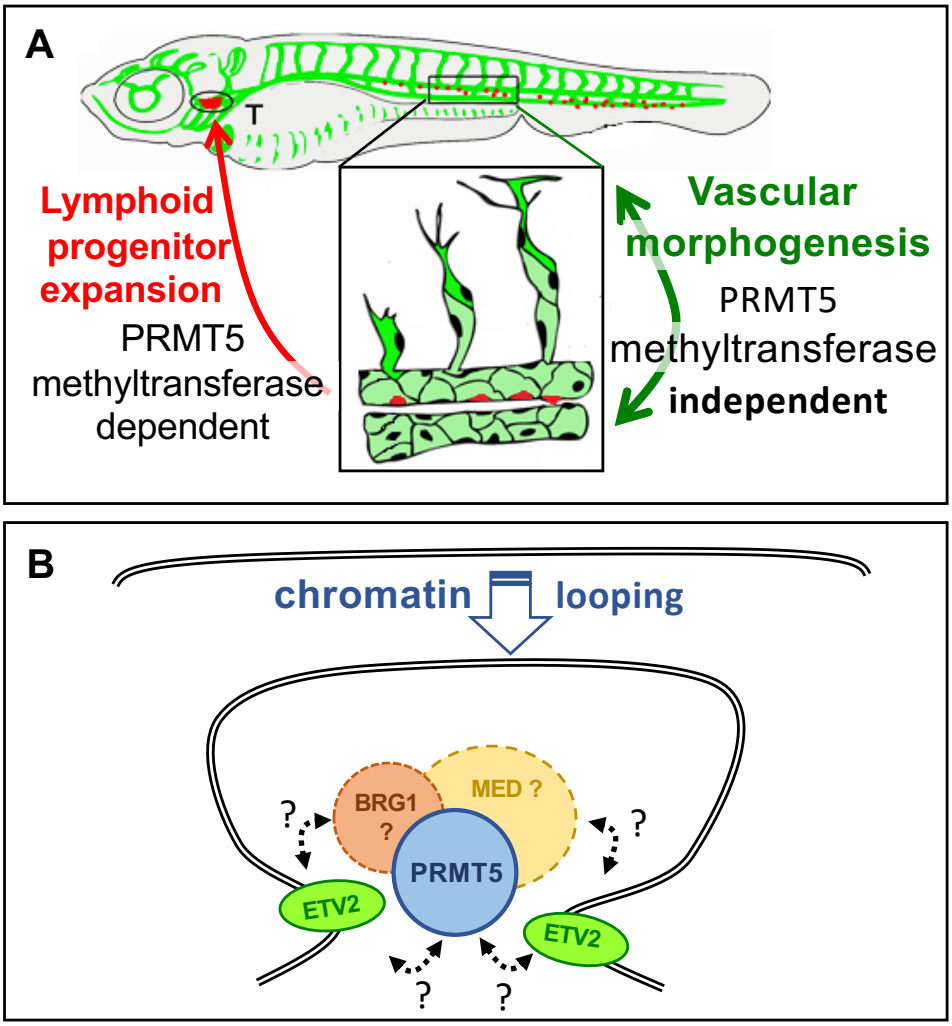
A
T
Lymphoid progenitor expansion
PRMT5 methyltransferase dependent
Vascular morphogenesis
PRMT5 methyltransferase independent
B
chromatin
looping
BRG1 ?
MED ?
PRMT5
ETV2
ETV2
?
?
?
?

figureS1

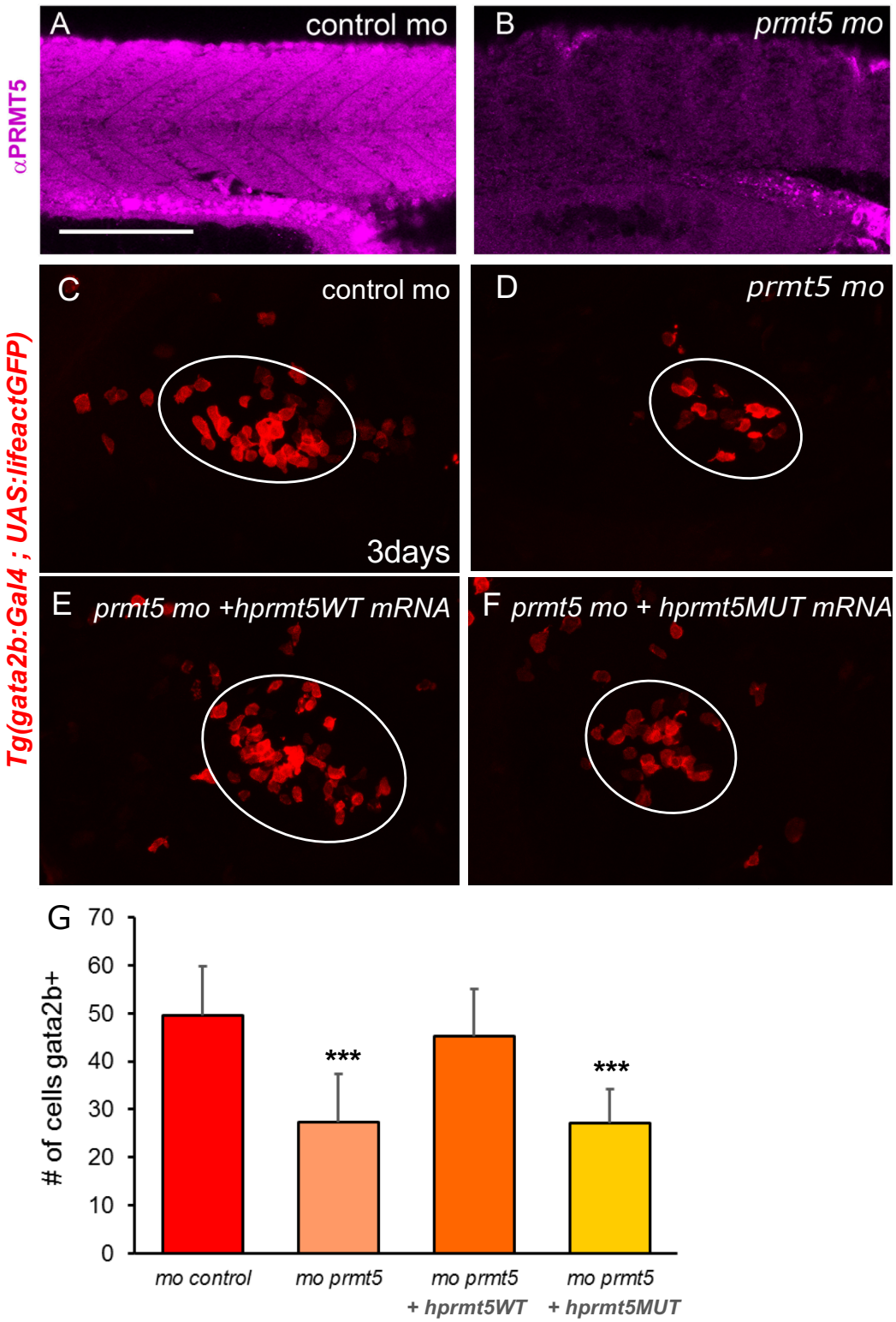
αPRMT5
A
control mo
B
prmt5 mo
Tg(gata2b:Gal4 ; UAS:lifeactGFP)
C
control mo
3days
D
prmt5 mo
E
prmt5 mo +hprmt5WT mRNA
F
prmt5 mo + hprmt5MUT mRNA
G
# of cells gata2b+
70
60
50
40
30
20
10
0
***
***
mo control
mo prmt5
mo prmt5
+ hprmt5WT
mo prmt5
+ hprmt5MUT

figure S2

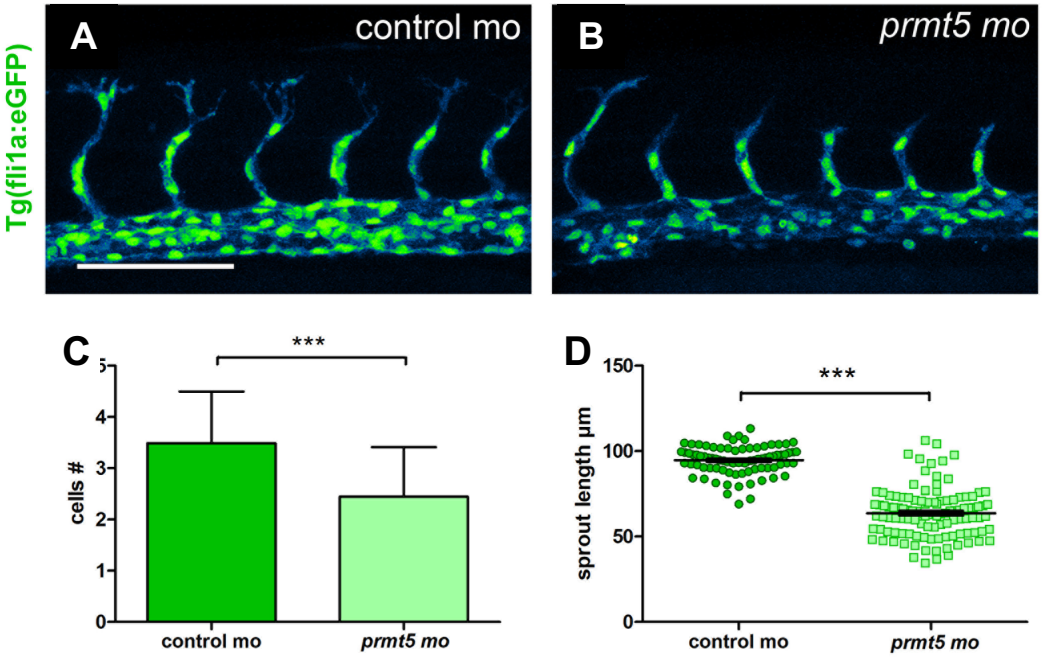
A
control mo
B
prmt5 mo
Tg(fli1a:eGFP)
C
***
cells #
0
1
2
3
4
5
control mo
prmt5 mo
D
***
sprout length µm
0
50
100
150
control mo
prmt5 mo

figure S3

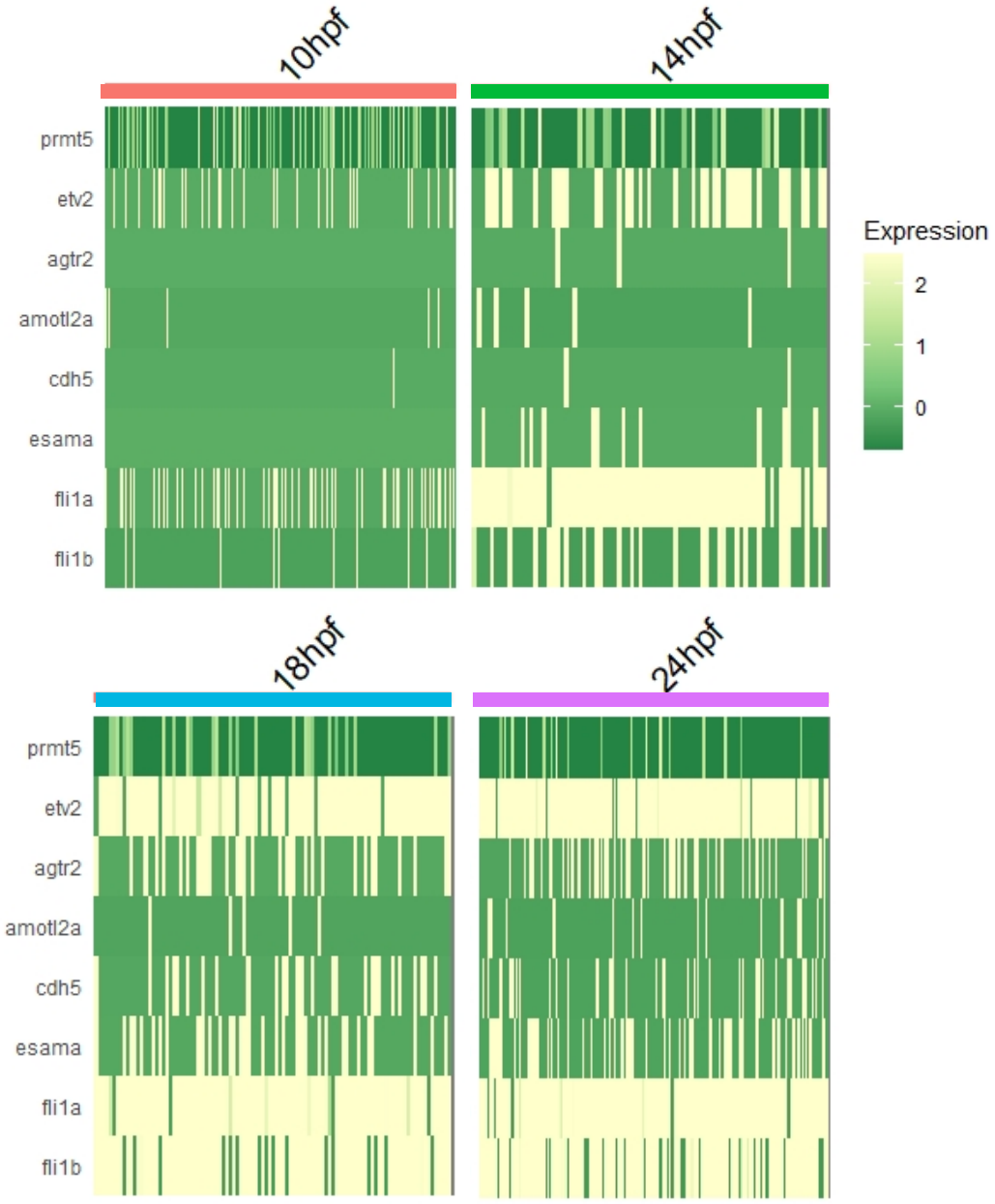
10hpf
14hpf
18hpf
24hpf
prmt5
etv2
agtr2
amotl2a
cdh5
esama
fli1a
fli1b
Expression
2
1
0

figure S4

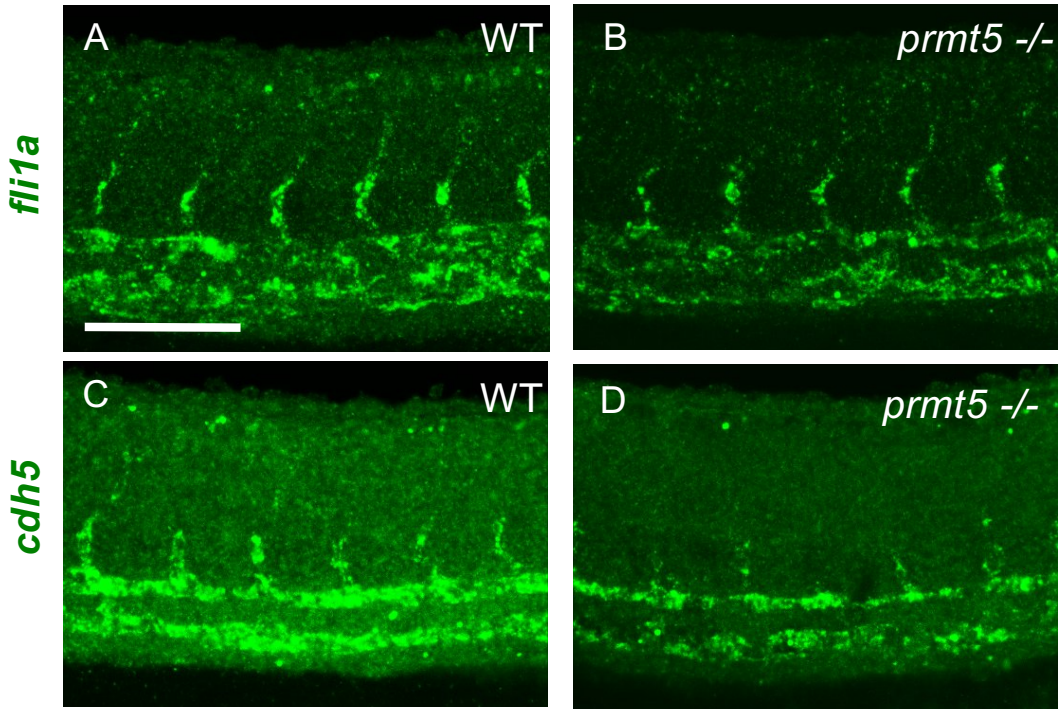
fli1a
cdh5
A
WT
B
prmt5 -/-
C
WT
D
prmt5 -/-

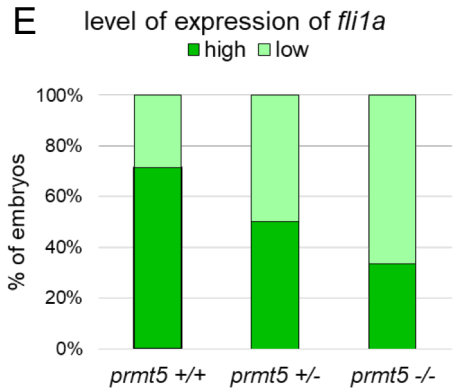
E
level of expression of fli1a
high
low
% of embryos
100%
80%
60%
40%
20%
0%
prmt5 +/+
prmt5 +/-
prmt5 -/-

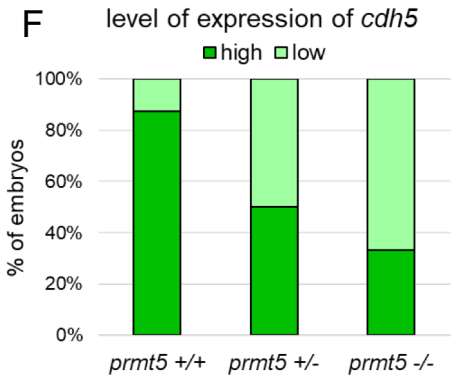
F
level of expression of cdh5
high
low
% of embryos
100%
80%
60%
40%
20%
0%
prmt5 +/+
prmt5 +/-
prmt5 -/-

figure S5

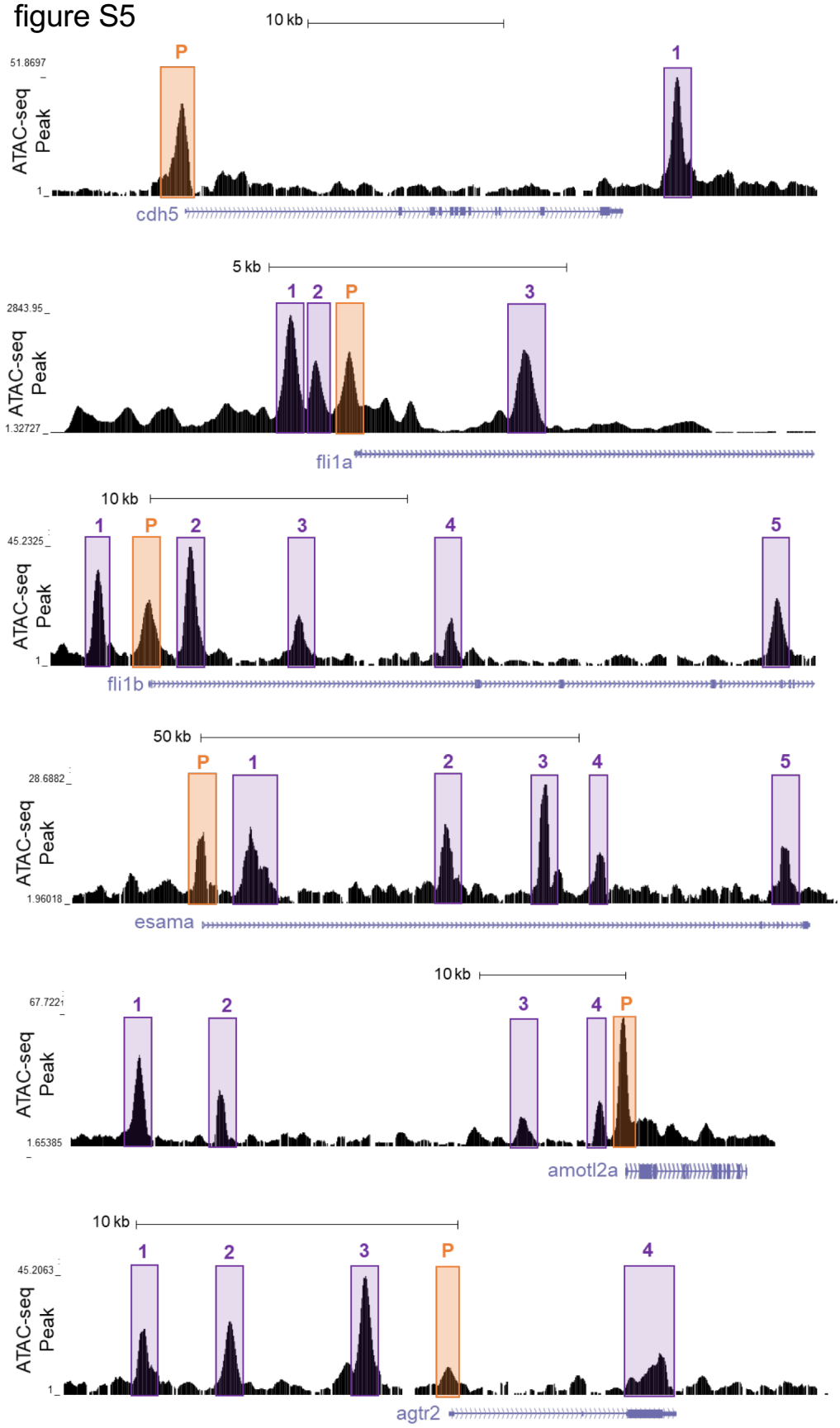
10 kb
51.8697
ATAC-seq
Peak
1
P
1
cdh5
5 kb
2843.95
1.32727
1
2
P
3
fli1a
10 kb
45.2325
1
1
P
2
3
4
5
fli1b
50 kb
28.6882
1.96018
P
1
2
3
4
5
esama
10 kb
67.722
1.65385
1
2
3
4
P
amotl2a
10 kb
45.2063
1
1
2
3
P
4
agtr2

Gene symbol	Peak chr	Peak start	Peak stop	ATAC-seq peak ID (fig. S5)	Distance of peakcenter to TSS
fli1a	*chr18*	*46991096*	*46991446*	*1*	*1 125*
fli1a	*chr18*	*46991648*	*46991909*	*2*	*663*
fli1a	*chr18*	*46992111*	*46992384*	*p*	*0*
fli1a	*chr18*	*46994744*	*46995457*	*3*	*2 866*
fli1b	*chr16*	*44785440*	*44785639*	*1*	*1 971*
fli1b	*chr16*	*44787371*	*44787644*	*p*	*0*
fli1b	*chr16*	*44788987*	*44789387*	*2*	*1 586*
fli1b	*chr16*	*44793201*	*44793495*	*3*	*5 851*
fli1b	*chr16*	*44799123*	*44799348*	*4*	***11 640***
fli1b	*chr16*	*44811618*	*44812080*	*5*	***24 462***
esama	*chr10*	*32600339*	*32600842*	*p*	*0*
esama	*chr10*	*32607536*	*32607916*	*1*	*6 894*
esama	*chr10*	*32632710*	*32633102*	*2*	***32 357***
esama	*chr10*	*32645662*	*32646247*	*3*	***45 230***
esama	*chr10*	*32653326*	*32653687*	*4*	***52 511***
esama	*chr10*	*32677711*	*32677978*	*5*	***76 617***
amotl2a	*chr6*	*27670527*	*27671187*	*1*	***29 519***
amotl2a	*chr6*	*27675738*	*27676044*	*2*	***24 324***
amotl2a	*chr6*	*27693946*	*27694363*	*3*	*6 172*
amotl2a	*chr6*	*27698667*	*27698822*	*4*	*1 629*
amotl2a	*chr6*	*27699920*	*27700375*	*p*	*0*
cdh5	*chr7*	*45432986*	*45433605*	*p*	*0*
cdh5	*chr7*	*45458271*	*45458821*	*1*	***24 800***
agtr2	*chr5*	*24901724*	*24902030*	*1*	***9 766***
agtr2	*chr5*	*24904437*	*24904720*	*2*	*6 990*
agtr2	*chr5*	*24908159*	*24908311*	*3*	*3 233*
agtr2	*chr5*	*24908459*	*24909026*	*4*	*2 645*
agtr2	*chr5*	*24917551*	*24917707*	*p*	*0*
agtr2	*chr5*	*24917756*	*24918031*	*5*	*6 525*

Table S1-Chromatin profile of Prmt5 identified target genes in zebrafish

ATAC-seq identified open chromatin regions surrounding characterized Prmt5 target genes and their distance to corresponding TSS (Quillien et al. 2017).

Name/application	Sequence 5'-3'
sgRNA1-*zPrmt5*-Fwd	TAGGGGTGGAACAGCGGCATACAC
sgRNA1-*zPrmt5*-Rev	AAACGTGTATGCCGCTGTTCCACC
Genotyping-*zPrmt5*-Fwd	CAAGACCTGTCCTGTTTGATGA
Genotyping-*zPrmt5*-Rev	GTGACTTTGCAGGGTCCAGT
XhoI-promo*cdh5*-Fwd	CCGCTCGAGCCAGGGGCATTTATCTTGG
EcoRI-promo*cdh5*-Rev	CGGAATTCAACGATCGCATACCAGAGT
BsaI-distenh*cdh5*-Fwd	GTAACGGGTCTCCATGGGACAACAGTCAAAATGTAGC
BsaI-distenh*cdh5*-Rev	GTAACGGGTCTCCCTTACACTCGCATAACAATTTCCA
BamHI-*gal4VP16*-Fwd	CGGGATCCGCCACCATGAAGCTACTGTCTTCTATC
SpeI-*gal4VP16*-Rev	GGACTAGTCTACATATCCAGAGCGCCG
Scla-qPCR-Fwd	ATGGATGACCCTCCACAAAA
Scla-qPCR-Rev	TCCCGGTTTAGCTTCTCATC
runx1-qPCR-Fwd	ACACTGGCGCTGCAACAAG
runx1-qPCR-Rev	CATCATTTCCCGCCATCACT
cmyb-qPCR-Fwd	GAACGGCTACGGTGGCTGGAA
cmyb-qPCR-Rev	CAGAGTCCAGCGAAGGACTGT
EF1α-qPCR-Fwd	GCATACATCAAGAAGATCGGC
EF1α-qPCR-Rev	GCAGCCTTCTGTGCAGACTTTG
agtr2-qPCR-Fwd	GTCATGTGCAAGCTGTGTGG
agtr2-qPCR-Rev	AACACATGAACCAACCGGCC
esama-qPCR-Fwd	AGACACCGAGGAGGATCTGG
esama-qPCR-Rev	GCTGGGTTGGTGTTGTATCC
amotl2a-qPCR-Fwd	GGGCACTTTATGCTCAACTCTTG
amotl2a-qPCR-Rev	CGGCCTTGCTCTCGTCTT
fli1b-qPCR-Fwd	TTCCATCAGCAGTCGTCTTG
fli1b-qPCR-Rev	TAGTTCCCTCCCAGGTGATG
Etv2-qPCR-Fwd	TGCCTTTGGAGGAAGAAAGA
Etv2-qPCR-Rev	CTGTTGTTGGCAATCTGCTG
Cdh5-qPCR-Fwd	CGAGATTGCTGATGGAGGAACGCC
Cdh5-qPCR-Rev	TGGCGAGGAGGGCACTGACA
fli1a-qPCR-Fwd	CCAAACATGACGACCAATGAGA
fli1a-qPCR-Rev	GTGATCCGGAGACCACAGAGA

Table S2- Sequences of oligonucleotides used in this study